01 Jan 2023

Second Order, Unconditionally Stable, Linear Ensemble Algorithms for the Magnetohydrodynamics Equations

John Carter

Daozhi Han
Missouri University of Science and Technology, handaoz@mst.edu

Nan Jiang
Missouri University of Science and Technology, jiangn@mst.edu

Second Order, Unconditionally Stable, Linear Ensemble Algorithms for the Magnetohydrodynamics Equations

John Carter[1] · **Daozhi Han**[1] · **Nan Jiang**[2]

Abstract

We propose two unconditionally stable, linear ensemble algorithms with pre-computable shared coefficient matrices across different realizations for the magnetohydrodynamics equations. The viscous terms are treated by a standard perturbative discretization. The nonlinear terms are discretized fully explicitly within the framework of the generalized positive auxiliary variable approach (GPAV). Artificial viscosity stabilization that modifies the kinetic energy is introduced to improve accuracy of the GPAV ensemble methods. Numerical results are presented to demonstrate the accuracy and robustness of the ensemble algorithms.

1 Introduction

Magnetohydrodynamics (MHD) flow describes electrically conducting fluid moving through a magnetic field. It has important applications in fusion technology, submarine propulsion system, liquid metals in magnetic pumps, and so on. The mathematical model comprises the Navier–Stokes equations for fluid flow and Maxwell's equations for electromagnetics. In practical applications, the problem parameters such as viscosity and magnetic resistivity, external body forcing and initial conditions, are invariably subject to uncertainty. To quan-

✉ Daozhi Han
    handaoz@mst.edu

    John Carter
    jachdm@mst.edu

    Nan Jiang
    jiangn@ufl.edu

1   Department of Mathematics and Statistics, Missouri University of Science and Technology, Rolla, MO 65409, USA

2   Department of Mathematics, University of Florida, Gainesville, FL, USA

tify the impact of uncertainty and develop high-fidelity numerical simulations, one usually computes the flow ensembles in which the MHD equations are solved repeatedly with different inputs. The aim of this article is to develop efficient second-order accurate ensemble algorithms that are unconditionally stable and suitable for long-time simulations. Therefore we consider solving J times the following MHD equations: for $j = 1, 2, \ldots, J$,

$$
\begin{cases}
\boldsymbol{u}_{j,t} + \boldsymbol{u}_j \cdot \nabla \boldsymbol{u}_j - s\boldsymbol{B}_j \cdot \nabla \boldsymbol{B}_j - \nu_j \Delta \boldsymbol{u}_j + \nabla p_j = \boldsymbol{f}_j \text{ in } \Omega \times (0, T), \\
\nabla \cdot \boldsymbol{u}_j = 0, \text{ in } \Omega \times (0, T), \\
\boldsymbol{B}_{j,t} + \boldsymbol{u}_j \cdot \nabla \boldsymbol{B}_j - \boldsymbol{B}_j \cdot \nabla \boldsymbol{u}_j - \gamma_j \Delta \boldsymbol{B}_j + \nabla \lambda_j = \nabla \times \boldsymbol{g}_j \text{ in } \Omega \times (0, T), \\
\nabla \cdot \boldsymbol{B}_j = 0, \text{ in } \Omega \times (0, T), \\
\boldsymbol{u}_j(x, 0) = \boldsymbol{u}_j^0(x), \text{ in } \Omega, \quad \boldsymbol{B}_j(x, 0) = \boldsymbol{B}_j^0(x), \text{ in } \Omega.
\end{cases} \quad (1)
$$

Here $\boldsymbol{u}_j$ is the fluid velocity, p_j the pressure, $\boldsymbol{B}_j$ the magnetic field and λ_j is a Lagrange multiplier corresponding to the solenoidal constraint on $\boldsymbol{B}_j$ [1]. The body force $\boldsymbol{f}_j(x, t)$ and $\nabla \times \boldsymbol{g}_j$ are given, s is the coupling number, ν_j is the kinematic viscosity, and γ_j is the magnetic resistivity. Dirichlet boundary conditions will be imposed for both $\boldsymbol{u}_j$ and $\boldsymbol{B}_j$, though the numerical methods are also applicable to other boundary conditions including $\nabla \times \boldsymbol{B}_j = 0$ on $\partial \Omega$. Note that we have adopted an equivalent formulation of the MHD equations, cf. [1–4].

Ensemble methods have been extensively developed for solving the Navier–Stokes equations and related fluid models [5–14]. The central idea in these ensemble methods is a perturbative time discretization that utilizes the ensemble mean corrected by explicit treatment of the fluctuations in time marching of each realization. As a result, at each time step the coefficient matrix of the resulting linear systems is identical for all realizations, saving both storage and computational cost. Moreover, under some constraint on the time-step and the size of fluctuations it is shown that the ensemble algorithms are long-time stable. A similar ensemble method is developed in [15] and [16] for solving a reduced MHD system at low magnetic Reynolds number. Based on the Elsasser formulation [17] and the perturbative time discretization, a first-order decoupled and unconditionally stable ensemble algorithm is proposed and analyzed in [1, 4] for solving the full MHD model. An artificial eddy viscosity term is employed to ensure unconditional stability. Due to the usage of Elsasser variables, the method appears to be limited to the case of Dirichlet boundary conditions.

Further computational efficiency gains can be achieved by fully explicit discretization of the nonlinear terms so that the exact same coefficient matrix is shared across different time steps in ensemble simulations. This approach would often incur a CFL condition that hinders the efficiency of the algorithm for long-time simulation or for problems involving multiple scales. One remedy is the introduction of a Lagrange multiplier for enforcement of the underlying energy estimate (energy dissipation or conservation). This idea leads to recent development of the so-called Invariant Energy Quadratization (IEQ) method [18–21], and the Scalar Auxiliary Variable (SAV) approach [22, 23] for solving phase field models. Extensions of these methods are reported in [24–27] on the design of linear, decoupled, unconditionally stable numerical schemes for solving general nonlinear equations satisfying an energy law. Based on the SAV approach proposed in [24], a stabilized SAV ensemble algorithm is developed in [28] for parameterized flow problems where superior accuracy is observed thanks to a penalization of the kinetic energy causing the high frequency mode to quickly roll-off in the energy spectrum [29]. Stability and error analysis of a SAV method for the MHD equations is recently conducted in [30].

In this article we propose two linear, second-order accurate, unconditionally stable ensemble methods with shared coefficient matrix across different realizations and time steps for solving the MHD model. The parameters are treated by the usual perturbative method. We employ the Generalized Positive Auxiliary Variable framework (GPAV) from [25] in the discretization of the nonlinear terms. The advantages of the GPAV method include: linearity of the algebra equation for the scalar variable; provable positivity of the scalar variable; and flexibility in handling complex boundary conditions. These Lagrange multiplier type approaches often suffer from poor accuracy especially for long time simulation of advection-dominated flow, cf. [31] for a careful benchmark comparison study of the SAV approach. This drop in accuracy is also discussed and demonstrated in the numerical tests from [25]. In [32] a post-processing procedure is introduced to improve accuracy of the SAV method for the Cahn–Hilliard equation. In our method we adopt the stabilization technique of artificial viscosity that proves robust and efficient in past studies [28, 29]. The stabilization introduces a penalty term in the kinetic energy which leads to a quick roll-off of the under-resolved modes in the energy spectrum thus curtailing the inertial range and making the system more computable, cf. [29]. This mechanism is well-known in the Navier–Stokes-α model for large eddy simulation of turbulence [33, 34]. We perform extensive numerical tests to gauge the accuracy, efficiency and robustness of the proposed ensemble methods. Error analysis of the proposed numerical schemes is currently beyond scope of this article. Recent work on error analysis of finite element methods for MHD equations can be found in [35, 36]. See also [37, 38] for convergence analysis of numerical approximations to the Navier–Stokes equationswith nonsmooth initial data under low-regularity conditions.

To start, we define the ensemble mean and the fluctuation of the viscosity terms ν_j^n and the electric potential γ_j^n at timestep n respectively

$$\bar{\nu}^n = \frac{1}{J} \sum_{j=1}^{J} \nu_j^n \quad \text{and} \quad \bar{\gamma}^n = \frac{1}{J} \sum_{j=1}^{J} \gamma_j^n, \tag{mean}$$

$$\nu_j'^n = \nu_j^n - \bar{\nu}^n \quad \text{and} \quad \gamma_j'^n = \gamma_j^n - \bar{\gamma}^n, \ \nu'_{\max} = \max_j \max_{x \in \Omega} |\nu_j'^n(x)| \tag{fluctuation}$$

$$\text{and} \quad \gamma'_{\max} = \max_j \max_{x \in \Omega} |\gamma_j'^n(x)|,$$

where in our considerations $\nu_j^n = \nu_j, \gamma_j^n = \gamma_j$ are constants and $t_n = n\Delta t \ (n = 0, 1, 2, \ldots)$. Define

$$\mathbf{v}^{n+1/2} = \frac{1}{2}(\mathbf{v}^{n+1} + \mathbf{v}^n), \qquad \tilde{\mathbf{v}}^{n+1/2} = 2\mathbf{v}^{n-1/2} - \mathbf{v}^{n-3/2}, \tag{2}$$

$$\overset{*}{\tilde{\mathbf{v}}}^{n+1/2} = \frac{3}{2}\mathbf{v}^n - \frac{1}{2}\mathbf{v}^{n-1}, \qquad \tilde{\mathbf{v}}^{n+1} = 2\mathbf{v}^n - \mathbf{v}^{n-1}. \tag{3}$$

We define a shifted energy of the form

$$E_j(t) = E[\mathbf{u}_j, \mathbf{B}_j] = \int_\Omega \frac{1}{2}|\mathbf{u}_j|^2 d\Omega + \int_\Omega \frac{s}{2}|\mathbf{B}_j|^2 d\Omega + C_0, \tag{4}$$

where $E[\mathbf{u}_j, \mathbf{B}_j]$ is the total kinetic energy of the system, which for physical examples is bounded from below, and C_0 is an arbitrarily small positive constant chosen in such a way that $E_j(t) > 0$ for $0 \le t \le T$. Next, let $\mathscr{F}$ be any one-to-one increasing differentiable function with $\mathscr{F}^{-1} = \mathscr{G}$ such that

$$\begin{cases} \mathscr{F}(\chi) > 0, & \chi > 0, \tag{5} \\ \mathscr{G}(\chi) > 0, & \chi > 0. \tag{6} \end{cases}$$

The scalar variable $R_j(t)$ is defined by

$$R_j(t) = \mathcal{G}(E_j), \tag{7}$$
$$E_j(t) = \mathcal{F}(R_j). \tag{8}$$

With E_j as in (4), $R_j(t)$ then satisfies

$$\mathcal{F}'(R_j)\frac{dR_j}{dt} = \int_\Omega u_j \cdot \frac{\partial u_j}{\partial t} d\Omega + \int_\Omega sB_j \cdot \frac{\partial B_j}{\partial t} d\Omega. \tag{9}$$

Since $\frac{\mathcal{F}(R_j)}{E_j} = 1$ for all j, we may write

$$\mathcal{F}'(R_j)\frac{dR_j}{dt} = \int_\Omega \left[u_j \cdot \frac{\partial u_j}{\partial t} + sB_j \cdot \frac{\partial B_j}{\partial t} \right] d\Omega + \left[\frac{\mathcal{F}(R_j)}{E_j} - 1 \right]$$

$$\left[\int_\Omega u_j \cdot \left(v_j \Delta u_j - \nabla p_j + f_j \right) d\Omega \right.$$

$$+ \int_\Omega sB_j \cdot \left(\gamma_j \Delta B_j - \nabla \lambda_j + \nabla \times g_j \right) d\Omega \right]$$

$$+ \frac{\mathcal{F}(R_j)}{E_j} \left[\int_\Omega u_j \cdot [B_j \cdot \nabla B_j - u_j \cdot \nabla u_j] d\Omega \right.$$

$$- \int_\Omega u_j \cdot [B_j \cdot \nabla B_j - u_j \cdot \nabla u_j] d\Omega$$

$$+ \int_\Omega sB_j \cdot [B_j \cdot \nabla u_j - u_j \cdot \nabla B_j] d\Omega$$

$$- \int_\Omega sB_j \cdot [B_j \cdot \nabla u_j - u_j \cdot \nabla B_j] d\Omega \right]$$

$$= \int_\Omega \left[u_j \cdot \frac{\partial u_j}{\partial t} + sB_j \cdot \frac{\partial B_j}{\partial t} \right] d\Omega$$

$$- \int_\Omega u_j \cdot \left(v_j \Delta u_j - \nabla p_j + \frac{\mathcal{F}(R_j)}{E_j}[B_j \cdot \nabla B_j - u_j \cdot \nabla u_j] + f_j \right) d\Omega$$

$$- \int_\Omega sB_j \cdot \left(\gamma_j \Delta B_j - \nabla \lambda_j + \frac{\mathcal{F}(R_j)}{E_j}[B_j \cdot \nabla u_j - u_j \cdot \nabla B_j] + \nabla \times g_j \right) d\Omega$$

$$+ \frac{\mathcal{F}(R_j)}{E_j} \left[\int_\Omega u_j \cdot [B_j \cdot \nabla B_j - u_j \cdot \nabla u_j + v_j \Delta u_j - \nabla p_j + f_j] d\Omega \right.$$

$$+ \int_\Omega sB_j \cdot [B_j \cdot \nabla u_j - u_j \cdot \nabla B_j + \gamma_j \Delta B_j - \nabla \lambda_j + \nabla \times g_j] d\Omega \right] \tag{10}$$

Note that all the additional terms above amount to adding zero to (9). Using integration by parts we get the equality

$$\int_\Omega u_j \cdot [B_j \cdot \nabla B_j - u_j \cdot \nabla u_j + v_j \Delta u_j - \nabla p_j + f_j] d\Omega$$

$$+ \int_\Omega sB_j \cdot [B_j \cdot \nabla u_j - u_j \cdot \nabla B_j + \gamma_j \Delta B_j - \nabla \lambda_j + \nabla \times g_j] d\Omega$$

$$= -\int_\Omega (v_j |\nabla u_j|^2 + s\gamma_j |\nabla B_j|^2) d\Omega + \int_\Omega (f_j \cdot u_j + s(\nabla \times g_j) \cdot B_j) d\Omega + \int_\Gamma B_S(u_j, B_j) d\Gamma, \tag{11}$$

where $B_S(u_j, B_j)$ represents the forcing terms on the boundary, defined as

$$B_S(u_j, B_j) = \int_\Gamma \left(-\frac{1}{2}|u_j|^2 u_j - \frac{s}{2}|B_j|^2 u_j + v_j \nabla u_j \cdot u_j - p_j u_j \right.$$

$$+ s(\boldsymbol{B}_j \cdot \boldsymbol{u}_j)\boldsymbol{B}_j + s\gamma_j \nabla \boldsymbol{B}_j \cdot \boldsymbol{B}_j - s\lambda_j \boldsymbol{B}_j\Big) \cdot \hat{n} \, d\Gamma \tag{12}$$

and $\hat{n}$ is the unit normal vector to the boundary. We use this equality and write

$$\mathcal{F}'(R_j)\frac{dR_j}{dt} = \int_\Omega \left[\boldsymbol{u}_j \cdot \frac{\partial \boldsymbol{u}_j}{\partial t} + s\boldsymbol{B}_j \cdot \frac{\partial \boldsymbol{B}_j}{\partial t}\right]d\Omega$$

$$- \int_\Omega \boldsymbol{u}_j \cdot \left(\nu_j \Delta \boldsymbol{u}_j - \nabla p_j + \frac{\mathcal{F}(R_j)}{E_j}[\boldsymbol{B}_j \cdot \nabla \boldsymbol{B}_j - \boldsymbol{u}_j \cdot \nabla \boldsymbol{u}_j] + \boldsymbol{f}_j\right)d\Omega$$

$$- \int_\Omega s\boldsymbol{B}_j \cdot \left(\gamma_j \Delta \boldsymbol{B}_j - \nabla \lambda_j + \frac{\mathcal{F}(R_j)}{E_j}[\boldsymbol{B}_j \cdot \nabla \boldsymbol{u}_j - \boldsymbol{u}_j \cdot \nabla \boldsymbol{B}_j] + \nabla \times \boldsymbol{g}_j\right)d\Omega$$

$$+ \frac{\mathcal{F}(R_j)}{E_j}\left[-\int_\Omega (\nu_j|\nabla \boldsymbol{u}_j|^2 + s\gamma_j|\nabla \boldsymbol{B}_j|^2)d\Omega + \int_\Omega (\boldsymbol{f}_j \cdot \boldsymbol{u}_j + s(\nabla \times \boldsymbol{g}_j) \cdot \boldsymbol{B}_j)d\Omega \right.$$

$$\left. + \int_\Gamma B_S(\boldsymbol{u}_j, \boldsymbol{B}_j)d\Gamma \right]$$

$$+ \left[1 - \frac{\mathcal{F}(R_j)}{E_j}\right]\left| \int_\Omega (\boldsymbol{f}_j \cdot \boldsymbol{u}_j + s(\nabla \times \boldsymbol{g}_j) \cdot \boldsymbol{B}_j)d\Omega \right.$$

$$\left. + \int_\Gamma B_S(\boldsymbol{u}_j, \boldsymbol{B}_j)d\Gamma \right|, \tag{13}$$

As will be seen later, we consider this reformulation (including the addition of the terms within absolute value brackets) as a means of constructing numerical schemes that inherit unconditional stability with respect to the modified energy $\mathcal{F}(R_j)$ and guaranteed positivity of a computed scalar variable ξ_j to be defined.

With Dirichlet boundary conditions, a Crank-Nicolson scheme for 1 becomes

Algorithm 1 *Given $\boldsymbol{u}_j^n$, $\boldsymbol{B}_j^n$, p_j^n and λ_j^n, find $\boldsymbol{u}_j^{n+1}$, $\boldsymbol{B}_j^{n+1}$, p_j^{n+1} and λ_j^{n+1} satisfying*

$$\left(\frac{\boldsymbol{u}_j^{n+1} - \boldsymbol{u}_j^n}{\Delta t}\right) = -\xi_j \left(\tilde{\boldsymbol{u}}_j^{n+1/2} \cdot \nabla\right)\tilde{\boldsymbol{u}}_j^{n+1/2}$$

$$+ s\xi_j \left(\tilde{\boldsymbol{B}}_j^{n+1/2} \cdot \nabla\right)\tilde{\boldsymbol{B}}_j^{n+1/2} + \bar{\nu}^n \Delta \boldsymbol{u}_j^{n+1/2} \tag{14}$$

$$+ \nu_j'^n \Delta \tilde{\boldsymbol{u}}_j^{n+1/2} - \nabla p_j^{n+1/2} + \boldsymbol{f}_j^{n+1/2},$$

$$\nabla \cdot \boldsymbol{u}_j^{n+1} = 0, \tag{15}$$

$$\left(\frac{\boldsymbol{B}_j^{n+1} - \boldsymbol{B}_j^n}{\Delta t}\right) = \xi_j \left(\tilde{\boldsymbol{B}}_j^{n+1/2} \cdot \nabla\right)\tilde{\boldsymbol{u}}_j^{n+1/2}$$

$$- \xi_j \left(\tilde{\boldsymbol{u}}_j^{n+1/2} \cdot \nabla\right)\tilde{\boldsymbol{B}}_j^{n+1/2} + \bar{\gamma}^n \Delta \boldsymbol{B}_j^{n+1/2} \tag{16}$$

$$+ \gamma_j'^n \Delta \tilde{\boldsymbol{B}}_j^{n+1/2} - \nabla \lambda_j^{n+1/2} + \nabla \times \boldsymbol{g}_j^{n+1/2},$$

$$\nabla \cdot \boldsymbol{B}_j^{n+1}z = 0, \tag{17}$$

$$\xi_j = \frac{\mathcal{F}(R_j^{n+1})}{E(\bar{\boldsymbol{u}}_j^{n+1}, \bar{\boldsymbol{B}}_j^{n+1})}, \tag{18}$$

$$E(\bar{\boldsymbol{u}}_j^{n+1}, \bar{\boldsymbol{B}}_j^{n+1}) = \frac{1}{2}\|\bar{\boldsymbol{u}}_j^{n+1}\|^2 + \frac{s}{2}\|\bar{\boldsymbol{B}}_j^{n+1}\|^2 + C_0, \tag{19}$$

$$
\frac{\mathscr{F}(R_j^{n+1}) - \mathscr{F}(R_j^n)}{\Delta t} = \int_\Omega \boldsymbol{u}_j^{n+1/2} \cdot \left(\frac{\boldsymbol{u}_j^{n+1} - \boldsymbol{u}_j^n}{\Delta t} \right) d\Omega
$$

$$
+ \int_\Omega s \boldsymbol{B}_j^{n+1/2} \cdot \left(\frac{\boldsymbol{B}_j^{n+1} - \boldsymbol{B}_j^n}{\Delta t} \right) d\Omega
$$

$$
- \int_\Omega \boldsymbol{u}_j^{n+1/2} \cdot \left[- \xi_j \left(\tilde{\boldsymbol{u}}_j^{n+1/2} \cdot \nabla \right) \tilde{\boldsymbol{u}}_j^{n+1/2} + s\xi_j \left(\tilde{\boldsymbol{B}}_j^{n+1/2} \cdot \nabla \right) \tilde{\boldsymbol{B}}_j^{n+1/2} \right.
$$

$$
\left. + \bar{v}^n \Delta \boldsymbol{u}_j^{n+1/2} + v_j'^n \Delta \tilde{\boldsymbol{u}}_j^{n+1/2} - \nabla p_j^{n+1/2} + \boldsymbol{f}_j^{n+1/2} \right] d\Omega
$$

$$
- \int_\Omega s \boldsymbol{B}_j^{n+1/2} \cdot \left[\xi_j \left(\tilde{\boldsymbol{B}}_j^{n+1/2} \cdot \nabla \right) \tilde{\boldsymbol{u}}_j^{n+1/2} - \xi_j \left(\tilde{\boldsymbol{u}}_j^{n+1/2} \cdot \nabla \right) \tilde{\boldsymbol{B}}_j^{n+1/2} \right.
$$

$$
\left. + \bar{\gamma}^n \Delta \boldsymbol{B}_j^{n+1/2} + \gamma_j'^n \Delta \tilde{\boldsymbol{B}}_j^{n+1/2} - \nabla \lambda_j^{n+1/2} + \nabla \times \boldsymbol{g}_j^{n+1/2} \right] d\Omega
$$

$$
+ \xi_j \left[- \int_\Omega \left(v_j |\nabla \bar{\boldsymbol{u}}_j^{n+1/2}|^2 + s\gamma_j |\nabla \bar{\boldsymbol{B}}_j^{n+1/2}|^2 \right) d\Omega \right.
$$

$$
+ \int_\Omega \boldsymbol{f}_j^{n+1/2} \cdot \bar{\boldsymbol{u}}_j^{n+1/2} d\Omega
$$

$$
\left. + \int_\Omega s(\nabla \times \boldsymbol{g}_j^{n+1/2}) \cdot \bar{\boldsymbol{B}}_j^{n+1/2} d\Omega + \int_\Gamma B_S(\bar{\boldsymbol{u}}_j^{n+1/2}, \bar{\boldsymbol{B}}_j^{n+1/2}) d\Gamma \right]
$$

$$
+ (1 - \xi_j) \left| \int_\Omega \boldsymbol{f}_j^{n+1/2} \cdot \bar{\boldsymbol{u}}_j^{n+1/2} d\Omega \right.
$$

$$
\left. + \int_\Omega s(\nabla \times \boldsymbol{g}_j^{n+1/2}) \cdot \bar{\boldsymbol{B}}_j^{n+1/2} d\Omega + \int_\Gamma B_S(\bar{\boldsymbol{u}}_j^{n+1/2}, \bar{\boldsymbol{B}}_j^{n+1/2}) d\Gamma \right|.
\tag{20}
$$

Here $\bar{\boldsymbol{u}}_j^{n+1}$, $\bar{\boldsymbol{u}}_j^{n+1/2}$, $\bar{\boldsymbol{B}}_j^{n+1}$ and $\bar{\boldsymbol{B}}_j^{n+1/2}$ are second order approximations of $\boldsymbol{u}_j^{n+1}$, $\boldsymbol{u}_j^{n+1/2}$, $\boldsymbol{B}_j^{n+1}$, and $\boldsymbol{B}_j^{n+1/2}$ that will be defined later.

Again for Dirichlet boundary conditions, a BDF2 scheme is

Algorithm 2 Given $\boldsymbol{u}_j^{n-1}$, $\boldsymbol{u}_j^n$, $\boldsymbol{B}_j^{n-1}$, $\boldsymbol{B}_j^n$, find $\boldsymbol{u}_j^{n+1}$, $\boldsymbol{B}_j^{n+1}$, p_j^{n+1} and λ_j^{n+1} satisfying

$$
\left(\frac{3\boldsymbol{u}_j^{n+1} - 4\boldsymbol{u}_j^n + \boldsymbol{u}_j^{n-1}}{2\Delta t} \right) = -\xi_j \left(\tilde{\boldsymbol{u}}_j^{n+1} \cdot \nabla \right) \tilde{\boldsymbol{u}}_j^{n+1}
$$

$$
+ s\xi_j \left(\tilde{\boldsymbol{B}}_j^{n+1} \cdot \nabla \right) \tilde{\boldsymbol{B}}_j^{n+1} + \bar{v}^n \Delta \boldsymbol{u}_j^{n+1} + v_j'^n \Delta \tilde{\boldsymbol{u}}_j^{n+1} - \nabla p_j^{n+1} + \boldsymbol{f}_j^{n+1}
\tag{21}
$$

$$
\nabla \cdot \boldsymbol{u}_j^{n+1} = 0,
\tag{22}
$$

$$
\left(\frac{3\boldsymbol{B}_j^{n+1} - 4\boldsymbol{B}_j^n + \boldsymbol{B}_j^{n-1}}{2\Delta t} \right)
$$

$$
= \xi_j \left(\tilde{\boldsymbol{B}}_j^{n+1} \cdot \nabla \right) \tilde{\boldsymbol{u}}_j^{n+1} - \xi_j \left(\tilde{\boldsymbol{u}}_j^{n+1} \cdot \nabla \right) \tilde{\boldsymbol{B}}_j^{n+1} + \bar{\gamma}^n \Delta \boldsymbol{B}_j^{n+1}
\tag{23}
$$

$$
+ \gamma_j'^n \Delta \tilde{\boldsymbol{B}}_j^{n+1} - \nabla \lambda_j^{n+1} + \nabla \times \boldsymbol{g}_j^{n+1},
$$

$$
\nabla \cdot \boldsymbol{B}_j^{n+1} = 0,
\tag{24}
$$

$$\xi_j = \frac{\mathscr{F}(\overset{*}{R}_j^{n+3/2})}{E(\bar{\boldsymbol{u}}_j^{n+3/2}, \bar{\boldsymbol{B}}_j^{n+3/2})}, \tag{25}$$

$$E(\bar{\boldsymbol{u}}_j^{n+3/2}, \bar{\boldsymbol{B}}_j^{n+3/2}) = \frac{1}{2}\|\bar{\boldsymbol{u}}_j^{n+3/2}\|^2 + \frac{s}{2}\|\bar{\boldsymbol{B}}_j^{n+3/2}\|^2 + C_0, \tag{26}$$

$$\frac{\mathscr{F}(\overset{*}{R}_j^{n+3/2}) - \mathscr{F}(\overset{*}{R}_j^{n+1/2})}{\Delta t} = \int_\Omega \boldsymbol{u}_j^{n+1} \cdot \left(\frac{3\boldsymbol{u}_j^{n+1} - 4\boldsymbol{u}_j^n + \boldsymbol{u}_j^{n-1}}{2\Delta t}\right) d\Omega$$

$$+ \int_\Omega s\boldsymbol{B}_j^{n+1} \cdot \left(\frac{3\boldsymbol{B}_j^{n+1} - 4\boldsymbol{B}_j^n + \boldsymbol{B}_j^{n-1}}{2\Delta t}\right) d\Omega$$

$$- \int_\Omega \boldsymbol{u}_j^{n+1} \cdot \Bigg[-\xi_j\left(\tilde{\boldsymbol{u}}_j^{n+1} \cdot \nabla\right)\tilde{\boldsymbol{u}}_j^{n+1} + s\xi_j\left(\tilde{\boldsymbol{B}}_j^{n+1} \cdot \nabla\right)\tilde{\boldsymbol{B}}_j^{n+1}$$

$$+ \bar{\nu}^n \Delta\boldsymbol{u}_j^{n+1} + \nu_j'^n \Delta\tilde{\boldsymbol{u}}_j^{n+1} - \nabla p_j^{n+1} + \boldsymbol{f}_j^{n+1} \Bigg] d\Omega$$

$$- \int_\Omega s\boldsymbol{B}_j^{n+1} \cdot \Bigg[\xi_j\left(\tilde{\boldsymbol{B}}_j^{n+1} \cdot \nabla\right)\tilde{\boldsymbol{u}}_j^{n+1} - \xi_j\left(\tilde{\boldsymbol{u}}_j^{n+1} \cdot \nabla\right)\tilde{\boldsymbol{B}}_j^{n+1}$$

$$+ \bar{\gamma}^n \Delta\boldsymbol{B}_j^{n+1} + \gamma_j'^n \Delta\tilde{\boldsymbol{B}}_j^{n+1} - \nabla\lambda_j^{n+1} + \nabla \times \boldsymbol{g}_j^{n+1} \Bigg] d\Omega$$

$$+ \xi_j\Bigg[-\int_\Omega \left(\nu_j|\nabla\bar{\boldsymbol{u}}_j^{n+1}|^2 + s\gamma_j|\nabla\bar{\boldsymbol{B}}_j^{n+1}|^2\right) d\Omega + \int_\Omega \boldsymbol{f}_j^{n+1} \cdot \bar{\boldsymbol{u}}_j^{n+1} d\Omega$$

$$+ \int_\Omega s(\nabla \times \boldsymbol{g}_j^{n+1}) \cdot \bar{\boldsymbol{B}}_j^{n+1} d\Omega + \int_\Gamma B_S(\bar{\boldsymbol{u}}_j^{n+1}, \bar{\boldsymbol{B}}_j^{n+1}) d\Gamma \Bigg]$$

$$+ (1 - \xi_j)\Bigg| \int_\Omega \boldsymbol{f}_j^{n+1} \cdot \bar{\boldsymbol{u}}_j^{n+1} d\Omega + \int_\Omega s(\nabla \times \boldsymbol{g}_j^{n+1}) \cdot \bar{\boldsymbol{B}}_j^{n+1} d\Omega$$

$$+ \int_\Gamma B_S(\bar{\boldsymbol{u}}_j^{n+1}, \bar{\boldsymbol{B}}_j^{n+1}) d\Gamma \Bigg|. \tag{27}$$

Similarly $\bar{\boldsymbol{u}}_j^{n+1}$, $\bar{\boldsymbol{u}}_j^{n+3/2}$, $\bar{\boldsymbol{B}}_j^{n+1}$ and $\bar{\boldsymbol{B}}_j^{n+3/2}$ are second order approximations of $\boldsymbol{u}_j^{n+1}$, $\boldsymbol{u}_j^{n+3/2}$, $\boldsymbol{B}_j^{n+1}$, and $\boldsymbol{B}_j^{n+3/2}$ to be defined later.

In practice, $(u_j^0, u_j^1, B_j^0, B_j^1)$ may be found from the initial conditions and using an algorithm without SAV, such as the aforementioned ensemble scheme in [1]. In our implementations, we used a primitive (without ensemble) first order scheme to initialize as the computational cost of solving each perturbation in these first steps is not significant.

The rest of the paper is outlined here. Section 2 gives mathematical preliminaries and defines notation. In Sect. 3, we prove the long time stability of the proposed algorithm. Section 4 presents an efficient way to implement our numerical algorithm. Section 5 numerically tests the proposed algorithm and illustrates theoretical results. Final conclusions and future directions are discussed in Sect. 5.

2 Notation and Preliminaries

Throughout this paper the $L^2(\Omega)$ norm of scalars, vectors, and tensors will be denoted by $\|\cdot\|$ with the usual L^2 inner product denoted by $(\cdot, \cdot)$. $H^k(\Omega)$ is the Sobolev space $W_2^k(\Omega)$, with

norm $\| \cdot \|_k$. For functions $v(x, t)$ defined on $(0, T)$, we define the norms, for $1 \le m < \infty$,

$$\|v\|_{\infty,k} := EssSup_{[0,T]}\|v(\cdot, t)\|_k \quad \text{and} \quad \|v\|_{m,k} := \left(\int_0^T \|v(\cdot, t)\|_k^m \, dt \right)^{1/m}.$$

The function spaces we consider are:

$$X := H_0^1(\Omega)^d = \left\{ v \in L^2(\Omega)^d : \nabla v \in L^2(\Omega)^{d \times d} \text{ and } v = 0 \text{ on } \partial\Omega \right\},$$

$$Q := L_0^2(\Omega) = \left\{ q \in L^2(\Omega) : \int_\Omega q \, dx = 0 \right\},$$

$$V := \{ v \in X : (\nabla \cdot v, q) = 0, \forall q \in Q \}.$$

A weak formulation of the full MHD equations is: Find $u_j : [0, T] \to X$, $p_j : [0, T] \to Q$, $B_j : [0, T] \to X$ and $\lambda_j : [0, T] \to Q$ satisfying

$$(u_{j,t}, v) + (u_j \cdot \nabla u_j, v) - s(B_j \cdot \nabla B_j, v) + v_j(\nabla u_j, \nabla v) - (p_j, \nabla \cdot v) = (f_j, v), \quad \forall v \in X,$$

$$(\nabla \cdot u_j, l) = 0, \quad \forall l \in Q,$$

$$(B_{j,t}, \chi) + (u_j \cdot \nabla B_j, \chi) - (B_j \cdot \nabla u_j, \chi) + \gamma_j(\nabla B_j, \nabla \chi) - (\lambda_j, \nabla \cdot \chi)$$
$$= (\nabla \times g_j, \chi), \quad \forall \chi \in X,$$

$$(\nabla \cdot B_j, \psi) = 0, \quad \forall \psi \in Q.$$

We denote conforming velocity, pressure, potential finite element spaces based on an edge to edge triangulation ($d = 2$) or tetrahedralization ($d = 3$) of Ω with maximum element diameter h by

$$X_h \subset X, \ Q_h \subset Q.$$

We also assume the finite element spaces (X_h, Q_h) satisfy the usual discrete inf-sup /LBB^h condition for stability of the discrete pressure, see [39] for more on this condition. Taylor–Hood elements, e.g., [39, 40], are one such choice used in the tests in Sect. 5. We define the trilinear form

$$b(u, v, w) := (u \cdot \nabla v, w)$$

The full discretization of the proposed partitioned ensemble algorithm with Crank–Nicolson scheme is

Algorithm 3 *Given $u_{j,h}^n$, $B_{j,h}^n$, $p_{j,h}^n$ and $\lambda_{j,h}^n$, find $u_{j,h}^{n+1}$, $B_{j,h}^{n+1}$, $p_{j,h}^{n+1}$ and $\lambda_{j,h}^{n+1}$ satisfying for any v_h, $\chi_h \in X_h$ and $l_h, \psi_h \in Q_h$,*

$$\left(\frac{u_{j,h}^{n+1} - u_{j,h}^n}{\Delta t}, v_h \right) = -\xi_j b(\tilde{u}_{j,h}^{n+1/2}, \tilde{u}_{j,h}^{n+1/2}, v_h) + s\xi_j b(\tilde{B}_{j,h}^{n+1/2}, \tilde{B}_{j,h}^{n+1/2}, v_h)$$

$$- \bar{v}^n \left(\nabla u_{j,h}^{n+1/2}, \nabla v_h \right) - v_j'^n \left(\nabla \tilde{u}_{j,h}^{n+1/2}, \nabla v_h \right) + \left(p_{j,h}^{n+1/2}, \nabla \cdot v_h \right)$$

$$- \alpha h \left(\nabla(u_{j,h}^{n+1} - u_{j,h}^n), \nabla v_h \right) + \left(f_{j,h}^{n+1/2}, v_h \right), \tag{28}$$

$$\left(\nabla \cdot u_{j,h}^{n+1}, l_h \right) = 0, \tag{29}$$

$$\left(\frac{B_{j,h}^{n+1} - B_{j,h}^n}{\Delta t}, \chi_h \right) = \xi_j b(\tilde{B}_{j,h}^{n+1/2}, \tilde{u}_{j,h}^{n+1/2}, \chi_h) - \xi_j b(\tilde{u}_{j,h}^{n+1/2}, \tilde{B}_{j,h}^{n+1/2}, \chi_h)$$

$$- \bar{\gamma}^n \left(\nabla B_{j,h}^{n+1/2}, \nabla \chi_h \right) - \gamma_j'^n \left(\nabla \tilde{B}_{j,h}^{n+1/2}, \nabla \chi_h \right) + \left(\lambda_{j,h}^{n+1/2}, \nabla \cdot \chi_h \right)$$

$$- \alpha_M h \left(\nabla (\boldsymbol{B}_{j,h}^{n+1} - \boldsymbol{B}_{j,h}^n), \nabla \boldsymbol{\chi}_h \right) + \left(\nabla \times \boldsymbol{g}_{j,h}^{n+1/2}, \boldsymbol{\chi}_h \right), \tag{30}$$

$$\left(\nabla \cdot \boldsymbol{B}_{j,h}^{n+1}, \psi_h \right) = 0, \tag{31}$$

$$\xi_j = \frac{\mathscr{F}(R_{j,h}^{n+1})}{E(\bar{\boldsymbol{u}}_{j,h}^{n+1}, \bar{\boldsymbol{B}}_{j,h}^{n+1})}, \tag{32}$$

$$E(\bar{\boldsymbol{u}}_{j,h}^{n+1}, \bar{\boldsymbol{B}}_{j,h}^{n+1}) = \frac{1}{2} \| \bar{\boldsymbol{u}}_{j,h}^{n+1} \|^2 + \frac{s}{2} \| \bar{\boldsymbol{B}}_{j,h}^{n+1} \|^2 + C_0, \tag{33}$$

$$\frac{\mathscr{F}(R_{j,h}^{n+1}) - \mathscr{F}(R_{j,h}^n)}{\Delta t} = \left(\frac{\boldsymbol{u}_{j,h}^{n+1} - \boldsymbol{u}_{j,h}^n}{\Delta t}, \boldsymbol{u}_{j,h}^{n+1/2} \right) + s \left(\frac{\boldsymbol{B}_{j,h}^{n+1} - \boldsymbol{B}_{j,h}^n}{\Delta t}, \boldsymbol{B}_{j,h}^{n+1/2} \right)$$

$$+ \xi_j b(\tilde{\boldsymbol{u}}_{j,h}^{n+1/2}, \tilde{\boldsymbol{u}}_{j,h}^{n+1/2}, \boldsymbol{u}_{j,h}^{n+1/2}) - s \xi_j b(\tilde{\boldsymbol{B}}_{j,h}^{n+1/2}, \tilde{\boldsymbol{B}}_{j,h}^{n+1/2}, \boldsymbol{u}_{j,h}^{n+1/2})$$

$$+ \bar{\nu}^n \| \nabla \boldsymbol{u}_{j,h}^{n+1/2} \|^2$$

$$+ \nu_j'^n \left(\nabla \tilde{\boldsymbol{u}}_{j,h}^{n+1/2}, \nabla \boldsymbol{u}_{j,h}^{n+1/2} \right) - \left(p_{j,h}^{n+1/2}, \nabla \cdot \boldsymbol{u}_{j,h}^{n+1/2} \right)$$

$$+ \alpha h \left(\nabla (\boldsymbol{u}_{j,h}^{n+1} - \boldsymbol{u}_{j,h}^n), \nabla \boldsymbol{u}_{j,h}^{n+1/2} \right) - \left(\boldsymbol{f}_{j,h}^{n+1/2}, \boldsymbol{u}_{j,h}^{n+1/2} \right)$$

$$- s \xi_j b(\tilde{\boldsymbol{B}}_{j,h}^{n+1/2}, \tilde{\boldsymbol{u}}_{j,h}^{n+1/2}, \boldsymbol{B}_{j,h}^{n+1/2}) + s \xi_j b(\tilde{\boldsymbol{u}}_{j,h}^{n+1/2}, \tilde{\boldsymbol{B}}_{j,h}^{n+1/2}, \boldsymbol{B}_{j,h}^{n+1/2})$$

$$+ s \bar{\gamma}^n \| \nabla \boldsymbol{B}_{j,h}^{n+1/2} \|^2$$

$$+ s \gamma_j'^n \left(\nabla \boldsymbol{B}_{j,h}^{n+1/2}, \nabla \boldsymbol{B}_{j,h}^{n+1/2} \right) - s \left(\lambda_{j,h}^{n+1/2}, \nabla \cdot \boldsymbol{B}_{j,h}^{n+1/2} \right)$$

$$+ s \alpha_M h \left(\nabla (\boldsymbol{B}_{j,h}^{n+1} - \boldsymbol{B}_{j,h}^n), \nabla \boldsymbol{B}_{j,h}^{n+1/2} \right)$$

$$- s \left(\nabla \times \boldsymbol{g}_{j,h}^{n+1/2}, \boldsymbol{B}_{j,h}^{n+1/2} \right) + \xi_j \left[- \int_\Omega \left(\nu_j | \nabla \bar{\boldsymbol{u}}_{j,h}^{n+1/2} |^2 \right. \right.$$

$$\left. + s \gamma_j | \nabla \bar{\boldsymbol{B}}_{j,h}^{n+1/2} |^2 \right) d\Omega$$

$$+ \int_\Omega \boldsymbol{f}_{j,h}^{n+1/2} \cdot \bar{\boldsymbol{u}}_{j,h}^{n+1/2} d\Omega + \int_\Omega s(\nabla \times \boldsymbol{g}_{j,h}^{n+1/2}) \cdot \bar{\boldsymbol{B}}_{j,h}^{n+1/2} d\Omega$$

$$+ \int_\Gamma B_S(\bar{\boldsymbol{u}}_{j,h}^{n+1/2}, \bar{\boldsymbol{B}}_{j,h}^{n+1/2}) d\Gamma \Bigg]$$

$$+ (1 - \xi_j) \left| \int_\Omega \boldsymbol{f}_{j,h}^{n+1/2} \cdot \bar{\boldsymbol{u}}_{j,h}^{n+1/2} d\Omega + \int_\Omega s(\nabla \times \boldsymbol{g}_{j,h}^{n+1/2}) \cdot \bar{\boldsymbol{B}}_{j,h}^{n+1/2} d\Omega \right.$$

$$+ \int_\Gamma B_S(\bar{\boldsymbol{u}}_{j,h}^{n+1/2}, \bar{\boldsymbol{B}}_{j,h}^{n+1/2}) d\Gamma \Bigg|. \tag{34}$$

The full discretization of the proposed partitioned ensemble algorithm with BDF2 scheme is

Algorithm 4 Given $\boldsymbol{u}_{j,h}^{n-1}, \boldsymbol{u}_{j,h}^n, \boldsymbol{B}_{j,h}^{n-1}, \boldsymbol{B}_{j,h}^n$, find $\boldsymbol{u}_{j,h}^{n+1}, \boldsymbol{B}_{j,h}^{n+1}, p_{j,h}^{n+1}$ and $\lambda_{j,h}^{n+1}$ satisfying for any $\boldsymbol{v}_h, \boldsymbol{\chi}_h \in X_h$ and $l_h, \psi_h \in Q_h$,

$$\left(\frac{3 \boldsymbol{u}_{j,h}^{n+1} - 4 \boldsymbol{u}_{j,h}^n + \boldsymbol{u}_{j,h}^{n-1}}{2 \Delta t}, \boldsymbol{v}_h \right) = - \xi_j b(\tilde{\boldsymbol{u}}_{j,h}^{n+1}, \tilde{\boldsymbol{u}}_{j,h}^{n+1}, \boldsymbol{v}_h) + s \xi_j b(\tilde{\boldsymbol{B}}_{j,h}^{n+1}, \tilde{\boldsymbol{B}}_{j,h}^{n+1}, \boldsymbol{v}_h)$$

$$- \bar{\nu}^n \left(\nabla \boldsymbol{u}_{j,h}^{n+1}, \nabla \boldsymbol{v}_h \right) - \nu_j'^n \left(\nabla \tilde{\boldsymbol{u}}_{j,h}^{n+1}, \nabla \boldsymbol{v}_h \right) + \left(p_{j,h}^{n+1}, \nabla \cdot \boldsymbol{v}_h \right)$$

$$- \alpha h \left(\nabla (3\boldsymbol{u}_{j,h}^{n+1} - 4\boldsymbol{u}_{j,h}^{n} + \boldsymbol{u}_{j,h}^{n-1}), \nabla \boldsymbol{v}_h \right) + \left(\boldsymbol{f}_{j,h}^{n+1}, \boldsymbol{v}_h \right), \tag{35}$$

$$\left(\nabla \cdot \boldsymbol{u}_{j,h}^{n+1}, l_h \right) = 0, \tag{36}$$

$$\left(\frac{3\boldsymbol{B}_{j,h}^{n+1} - 4\boldsymbol{B}_{j,h}^{n} + \boldsymbol{B}_{j,h}^{n-1}}{2\Delta t}, \boldsymbol{\chi}_h \right) = \xi_j b(\tilde{\boldsymbol{B}}_{j,h}^{n+1}, \tilde{\boldsymbol{u}}_{j,h}^{n+1}, \boldsymbol{\chi}_h) - \xi_j b(\tilde{\boldsymbol{u}}_{j,h}^{n+1}, \tilde{\boldsymbol{B}}_{j,h}^{n+1}, \boldsymbol{\chi}_h)$$

$$- \bar{\gamma}^n \left(\nabla \boldsymbol{B}_{j,h}^{n+1}, \nabla \boldsymbol{\chi}_h \right) - \gamma_j'^n \left(\nabla \tilde{\boldsymbol{B}}_{j,h}^{n+1}, \nabla \boldsymbol{\chi}_h \right) + \left(\lambda_{j,h}^{n+1}, \nabla \cdot \boldsymbol{\chi}_h \right)$$

$$- \alpha_M h \left(\nabla (3\boldsymbol{B}_{j,h}^{n+1} - 4\boldsymbol{B}_{j,h}^{n} + \boldsymbol{B}_{j,h}^{n-1}), \nabla \boldsymbol{\chi}_h \right) + \left(\nabla \times \boldsymbol{g}_{j,h}^{n+1}, \boldsymbol{\chi}_h \right), \tag{37}$$

$$\left(\nabla \cdot \boldsymbol{B}_{j,h}^{n+1}, \psi_h \right) = 0, \tag{38}$$

$$\xi_j = \frac{\mathscr{F}(\overset{*}{R}_{j,h}^{n+3/2})}{E(\bar{\boldsymbol{u}}_{j,h}^{n+3/2}, \bar{\boldsymbol{B}}_{j,h}^{n+3/2})}, \tag{39}$$

$$E(\bar{\boldsymbol{u}}_{j,h}^{n+3/2}, \bar{\boldsymbol{B}}_{j,h}^{n+3/2}) = \frac{1}{2} \|\bar{\boldsymbol{u}}_{j,h}^{n+3/2}\|^2 + \frac{s}{2} \|\bar{\boldsymbol{B}}_{j,h}^{n+3/2}\|^2 + C_0,$$

$$\frac{\mathscr{F}(\overset{*}{R}_{j,h}^{n+3/2}) - \mathscr{F}(\overset{*}{R}_{j,h}^{n+1/2})}{\Delta t} = \left(\frac{3\boldsymbol{u}_{j,h}^{n+1} - 4\boldsymbol{u}_{j,h}^{n} + \boldsymbol{u}_{j,h}^{n-1}}{2\Delta t}, \boldsymbol{u}_{j,h}^{n+1} \right) \tag{40}$$

$$+ s \left(\frac{3\boldsymbol{B}_{j,h}^{n+1} - 4\boldsymbol{B}_{j,h}^{n} + \boldsymbol{B}_{j,h}^{n-1}}{2\Delta t}, \boldsymbol{B}_{j,h}^{n+1} \right) + \xi_j b(\tilde{\boldsymbol{u}}_{j,h}^{n+1}, \tilde{\boldsymbol{u}}_{j,h}^{n+1}, \boldsymbol{u}_{j,h}^{n+1})$$

$$- s\xi_j b(\tilde{\boldsymbol{B}}_{j,h}^{n+1}, \tilde{\boldsymbol{B}}_{j,h}^{n+1}, \boldsymbol{u}_{j,h}^{n+1}) + \bar{\nu}^n \|\nabla \boldsymbol{u}_{j,h}^{n+1}\|^2 + \nu_j'^n \left(\nabla \tilde{\boldsymbol{u}}_{j,h}^{n+1}, \nabla \boldsymbol{u}_{j,h}^{n+1} \right)$$

$$- \left(p_{j,h}^{n+1}, \nabla \cdot \boldsymbol{u}_{j,h}^{n+1} \right) + \alpha h \left(\nabla (3\boldsymbol{u}_{j,h}^{n+1} - 4\boldsymbol{u}_{j,h}^{n} + \boldsymbol{u}_{j,h}^{n-1}), \nabla \boldsymbol{u}_{j,h}^{n+1} \right) - \left(\boldsymbol{f}_{j,h}^{n+1}, \boldsymbol{u}_{j,h}^{n+1} \right)$$

$$- s\xi_j b(\tilde{\boldsymbol{B}}_{j,h}^{n+1}, \tilde{\boldsymbol{u}}_{j,h}^{n+1}, \boldsymbol{B}_{j,h}^{n+1}) + s\xi_j b(\tilde{\boldsymbol{u}}_{j,h}^{n+1}, \tilde{\boldsymbol{B}}_{j,h}^{n+1}, \boldsymbol{B}_{j,h}^{n+1})$$

$$+ s\bar{\gamma}^n \|\nabla \boldsymbol{B}_{j,h}^{n+1}\|^2 + s\gamma_j'^n \left(\nabla \tilde{\boldsymbol{B}}_{j,h}^{n+1}, \nabla \boldsymbol{B}_{j,h}^{n+1} \right)$$

$$- s \left(\lambda_{j,h}^{n+1}, \nabla \cdot \boldsymbol{B}_{j,h}^{n+1} \right) + s\alpha_M h \left(\nabla (3\boldsymbol{B}_{j,h}^{n+1} - 4\boldsymbol{B}_{j,h}^{n} + \boldsymbol{B}_{j,h}^{n-1}), \nabla \boldsymbol{B}_{j,h}^{n+1} \right)$$

$$- s \left(\nabla \times \boldsymbol{g}_{j,h}^{n+1}, \boldsymbol{B}_{j,h}^{n+1} \right)$$

$$+ \xi_j \left[- \int_\Omega \left(\nu_j |\nabla \bar{\boldsymbol{u}}_{j,h}^{n+1}|^2 + s\gamma_j |\nabla \bar{\boldsymbol{B}}_{j,h}^{n+1}|^2 \right) d\Omega + \int_\Omega \boldsymbol{f}_{j,h}^{n+1} \cdot \bar{\boldsymbol{u}}_{j,h}^{n+1} d\Omega \right.$$

$$+ \int_\Omega s(\nabla \times \boldsymbol{g}_{j,h}^{n+1}) \cdot \bar{\boldsymbol{B}}_{j,h}^{n+1} d\Omega + \int_\Gamma B_S(\bar{\boldsymbol{u}}_{j,h}^{n+1}, \bar{\boldsymbol{B}}_{j,h}^{n+1}) d\Gamma \right]$$

$$+ (1 - \xi_j) \left| \int_\Omega \boldsymbol{f}_{j,h}^{n+1} \cdot \bar{\boldsymbol{u}}_{j,h}^{n+1} d\Omega + \int_\Omega s(\nabla \times \boldsymbol{g}_{j,h}^{n+1}) \cdot \bar{\boldsymbol{B}}_{j,h}^{n+1} d\Omega + \int_\Gamma B_S(\bar{\boldsymbol{u}}_{j,h}^{n+1}, \bar{\boldsymbol{B}}_{j,h}^{n+1}) d\Gamma \right|. \tag{41}$$

There's also the addition of two regularization terms in Algorithms (3) and (4),

$$\begin{cases} \alpha h \Delta(\boldsymbol{u}_{j,h}^{n+1} - \boldsymbol{u}_{j,h}^{n}), \\ \alpha_M h \Delta(\boldsymbol{B}_{j,h}^{n+1} - \boldsymbol{B}_{j,h}^{n}), \end{cases} \quad \text{for CN,} \qquad \begin{cases} \alpha h \Delta(3\boldsymbol{u}_{j,h}^{n+1} - 4\boldsymbol{u}_{j,h}^{n} + \boldsymbol{u}_{j,h}^{n-1}), \\ \alpha_M h \Delta(3\boldsymbol{B}_{j,h}^{n+1} - 4\boldsymbol{B}_{j,h}^{n} + \boldsymbol{B}_{j,h}^{n-1}), \end{cases} \quad \text{for BDF2.}$$

These terms are highly effective at reducing the considerable error that eventually appears when the timestep is not sufficiently refined. Significant improvement in accuracy will be seen later in the numerical tests. It's noted in [29] that this improvement cannot be explained by the stability or error analysis alone. Instead, an explanation is offered through analysis of a modified form of the equations under consideration. In the modified equations, the addition of the term $-\alpha h k \Delta u_t$ (in the case of velocity) and $-\alpha h k \Delta B_t$ (in the case of magnetic field) are added to the left-hand sides,

$$
\begin{cases}
\left[\boldsymbol{u}_{j,t} - \alpha h k \Delta \boldsymbol{u}_{j,t}\right] + \boldsymbol{u}_j \cdot \nabla \boldsymbol{u}_j - s\boldsymbol{B}_j \cdot \nabla \boldsymbol{B}_j - \nu_j \Delta \boldsymbol{u}_j + \nabla p_j = \boldsymbol{f}_j \text{ in } \Omega \times (0, T), \\
\nabla \cdot \boldsymbol{u}_j = 0, \text{ in } \Omega \times (0, T), \\
\left[\boldsymbol{B}_{j,t} - s\alpha_M h k \Delta \boldsymbol{B}_{j,t}\right] + \boldsymbol{u}_j \cdot \nabla \boldsymbol{B}_j - \boldsymbol{B}_j \cdot \nabla \boldsymbol{u}_j - \gamma_j \Delta \boldsymbol{B}_j + \nabla \lambda_j = \nabla \times \boldsymbol{g}_j \text{ in } \Omega \times (0, T), \\
\nabla \cdot \boldsymbol{B}_j = 0, \text{ in } \Omega \times (0, T), \\
\boldsymbol{u}_j(x, 0) = \boldsymbol{u}_j^0(x), \text{ in } \Omega, \quad \boldsymbol{B}_j(x, 0) = \boldsymbol{B}_j^0(x), \text{ in } \Omega.
\end{cases}
\tag{42}
$$

This results in a modified kinetic energy corresponding to the equation. In our case, the resulting modified kinetic energy would be

$$
\|u(t)\|^2 + \alpha h k \|\nabla u(t)\|^2 + s\|B(t)\|^2 + s\alpha_M h k \|\nabla B(t)\|^2.
$$

Following Kraichnan's theory [41], it is argued in [29] that the penalty term in the kinetic energy induces an enhanced energy decay rate for numerically under-resolved modes while preserving the correct energy cascade above the cut-off length scale. The quick roll-off in the energy spectrum is also exploited in the Navier–Stokes-α model (NS-α)—a nonlinearly dispersive modification of the Navier–Stokes equations for large eddy simulation of turbulence [33, 34]. This roll-off mechanism shortens the inertial range and makes the system more computable.

3 Stability of the Method

3.1 Crank–Nicolson

Theorem 5 *With homogeneous boundary conditions and forcing terms equal to zero, Algorithm (3) is unconditionally stable with respect to the modified energy $\mathscr{F}(R_j)$.*

Proof Stability follows directly from [25]. Set v_h to $\boldsymbol{u}_{j,h}^{n+1/2}$ in (28), χ_h to $s\boldsymbol{B}_{j,h}^{n+1/2}$ in (31), add each of these to (34) and note (29) and (32). Then one gets

$$
\mathscr{F}(R_{j,h}^{n+1}) - \mathscr{F}(R_{j,h}^n) = -\Delta t \frac{\mathscr{F}(R_{j,h}^{n+1})}{E\left(\bar{\boldsymbol{u}}_{j,h}^{n+1}, \bar{\boldsymbol{B}}_{j,h}^{n+1}\right)} \int_\Omega \left(\nu_j |\nabla \bar{\boldsymbol{u}}_{j,h}^{n+1/2}|^2 + s\gamma_j |\nabla \bar{\boldsymbol{B}}_{j,h}^{n+1/2}|^2\right) d\Omega
$$

$$
+ \left[1 - \frac{\mathscr{F}(R_{j,h}^{n+1})}{E\left(\bar{\boldsymbol{u}}_{j,h}^{n+1}, \bar{\boldsymbol{B}}_{j,h}^{n+1}\right)}\right] |S_0|\Delta t + \frac{\mathscr{F}(R_{j,h}^{n+1})}{E\left(\bar{\boldsymbol{u}}_{j,h}^{n+1}, \bar{\boldsymbol{B}}_{j,h}^{n+1}\right)} S_0 \Delta t.
\tag{43}
$$

Where $S_0 = \int_\Omega \boldsymbol{f}_{j,h}^{n+1/2} \cdot \bar{\boldsymbol{u}}_{j,h}^{n+1/2} d\Omega + \int_\Omega s(\nabla \times \boldsymbol{g}_{j,h}^{n+1/2}) \cdot \bar{\boldsymbol{B}}_{j,h}^{n+1/2} d\Omega$. Solving for $\mathscr{F}(R_{j,h}^{n+1})$ gives

$$\mathscr{F}(R_{j,h}^{n+1}) = \frac{\mathscr{F}(R_{j,h}^n) + |S_0|\Delta t}{1 + \frac{\Delta t}{E\left(\bar{\boldsymbol{u}}_{j,h}^{n+1}, \bar{\boldsymbol{B}}_{j,h}^{n+1}\right)} \left[\int_\Omega \left(\nu_j |\nabla \bar{\boldsymbol{u}}_{j,h}^{n+1/2}|^2 + s\gamma_j |\nabla \bar{\boldsymbol{B}}_{j,h}^{n+1/2}|^2\right) d\Omega + (|S_0| - S_0)\right]}. \tag{44}$$

If $\boldsymbol{f}_j = 0$ and $\nabla \times \boldsymbol{g}_j = 0$, then $S_0 = 0$ and

$$\mathscr{F}(R_{j,h}^{n+1}) = \frac{\mathscr{F}(R_{j,h}^n)}{1 + \frac{\Delta t}{E\left(\bar{\boldsymbol{u}}_{j,h}^{n+1}, \bar{\boldsymbol{B}}_{j,h}^{n+1}\right)} \int_\Omega \left(\nu_j |\nabla \bar{\boldsymbol{u}}_{j,h}^{n+1/2}|^2 + s\gamma_j |\nabla \bar{\boldsymbol{B}}_{j,h}^{n+1/2}|^2\right) d\Omega}. \tag{45}$$

Note the denominator in (45) is greater than or equal to 1. By definition (5), if $R_{j,h}^0 > 0$, then $\mathscr{F}(R_{j,h}^0) > 0$. In fact $R_{j,h}^0$ would be initialized as $\mathscr{G}\left(E[\boldsymbol{u}_j^0(x), \boldsymbol{B}_j^0(x)]\right)$, which by definition (6) is guaranteed positive. Then by induction for any timestep n, $\mathscr{F}(R_{j,h}^{n+1}) > 0$, giving us

$$0 < \mathscr{F}(R_{j,h}^{n+1}) \le \mathscr{F}(R_{j,h}^n), \qquad n \ge 0. \tag{46}$$

This completes the proof. $\square$

3.2 BDF2

Theorem 6 *With homogeneous boundary conditions and forcing terms equal to zero, Algorithm (4) is unconditionally stable with respect to the modified energy $\mathscr{F}(R_j)$ as long as the approximations of $R_j(t)$ at timestep $\frac{1}{2}$ are positive.*

Proof If one sets $\boldsymbol{v}_h$ to $\boldsymbol{u}_{j,h}^{n+1}$ in (35) and $\boldsymbol{\chi}_h$ to $s\boldsymbol{B}_{j,h}^{n+1}$ in (37), subtracts each of these from (41) and notes (36) and (38), the proof follows identically to [25]. We have

$$\mathscr{F}(\overset{*}{R}_{j,h}^{n+3/2}) - \mathscr{F}(\overset{*}{R}_{j,h}^{n+1/2}) = -\Delta t \frac{\mathscr{F}(\overset{*}{R}_{j,h}^{n+3/2})}{E(\bar{\boldsymbol{u}}_{j,h}^{n+3/2}, \bar{\boldsymbol{B}}_{j,h}^{n+3/2})} \int_\Omega \left(\nu_j |\nabla \bar{\boldsymbol{u}}_{j,h}^{n+1}|^2 + s\gamma_j |\nabla \bar{\boldsymbol{B}}_{j,h}^{n+1}|^2\right) d\Omega$$
$$+ \left[1 - \frac{\mathscr{F}(\overset{*}{R}_{j,h}^{n+3/2})}{E(\bar{\boldsymbol{u}}_{j,h}^{n+3/2}, \bar{\boldsymbol{B}}_{j,h}^{n+3/2})}\right] |S_0|\Delta t + \frac{\mathscr{F}(\overset{*}{R}_{j,h}^{n+3/2})}{E(\bar{\boldsymbol{u}}_{j,h}^{n+3/2}, \bar{\boldsymbol{B}}_{j,h}^{n+3/2})} S_0 \Delta t. \tag{47}$$

Where $S_0 = \int_\Omega \boldsymbol{f}_{j,h}^{n+1} \cdot \bar{\boldsymbol{u}}_{j,h}^{n+1} d\Omega + \int_\Omega s(\nabla \times \boldsymbol{g}_{j,h}^{n+1}) \cdot \bar{\boldsymbol{B}}_{j,h}^{n+1} d\Omega$. Solving for $\mathscr{F}(\overset{*}{R}_{j,h}^{n+3/2})$ gives

$$\mathscr{F}(\overset{*}{R}_{j,h}^{n+3/2}) = \frac{\mathscr{F}(\overset{*}{R}_{j,h}^{n+1/2}) + |S_0|\Delta t}{1 + \frac{\Delta t}{E(\bar{\boldsymbol{u}}_{j,h}^{n+3/2}, \bar{\boldsymbol{B}}_{j,h}^{n+3/2})}[\int_\Omega \left(\nu_j |\nabla \bar{\boldsymbol{u}}_{j,h}^{n+1}|^2 + s\gamma_j |\nabla \bar{\boldsymbol{B}}_{j,h}^{n+1}|^2\right) d\Omega + (|S_0| - S_0)]}. \tag{48}$$

If $\boldsymbol{f}_j = 0$ and $\nabla \times \boldsymbol{g}_j = 0$, then $S_0 = 0$ and

$$\mathscr{F}(\overset{*}{R}_{j,h}^{n+3/2}) = \frac{\mathscr{F}(\overset{*}{R}_{j,h}^{n+1/2})}{1 + \frac{\Delta t}{E(\bar{\boldsymbol{u}}_{j,h}^{n+3/2}, \bar{\boldsymbol{B}}_{j,h}^{n+3/2})} \int_\Omega \left(\nu_j |\nabla \bar{\boldsymbol{u}}_{j,h}^{n+1}|^2 + s\gamma_j |\nabla \bar{\boldsymbol{B}}_{j,h}^{n+1}|^2\right) d\Omega}. \tag{49}$$

The denominator above is greater than or equal to 1. Now by definition (5), if it's ensured the approximation of $R_j(t)$ at timestep $1/2$ is positive, i.e. $\overset{*}{R}_{j,h}^{1/2} > 0$, then $\mathscr{F}\left(\overset{*}{R}_{j,h}^{1/2}\right) > 0$. Then by induction for any timestep n, $\mathscr{F}\left(\overset{*}{R}_{j,h}^{n+3/2}\right) > 0$ and

$$0 < \mathscr{F}\left(\overset{*}{R}_{j,h}^{n+3/2}\right) \le \mathscr{F}\left(\overset{*}{R}_{j,h}^{n+1/2}\right), \qquad n \ge 0. \tag{50}$$

This completes the proof. □

Note that for the choice of $\mathscr{F}(\chi) = \chi^2 \ge 0$ for all $\chi \in (-\infty, \infty)$, (50) and unconditional stability will hold regardless of whether $\overset{*}{R}_{j,h}^{1/2} > 0$.

4 Implementation

Since the schemes are linear and the auxiliary variables are scalar functions of time variable, the resulting systems can be solved conveniently by superposition of a series of Stokes-type equations. We illustrate the idea by presenting the algorithms in strong form.

4.1 Crank–Nicolson

To efficiently implement Algorithm (1), we proceed in the following manner. Assume

$$u_j^{n+1} = \hat{u}_j^{n+1} + \xi_j \breve{u}_j^{n+1}, \qquad p_j^{n+1} = \hat{p}_j^{n+1} + \xi_j \breve{p}_j^{n+1},$$
$$B_j^{n+1} = \hat{B}_j^{n+1} + \xi_j \breve{B}_j^{n+1}, \qquad \lambda_j^{n+1} = \hat{\lambda}_j^{n+1} + \xi_j \breve{\lambda}_j^{n+1}.$$

Then solving Algorithm (1) is equivalent to solving the following subproblems,

Algorithm 7 *Given u_j^{n-2}, u_j^{n-1}, u_j^n, B_j^{n-2}, B_j^{n-1}, B_j^n, p_j^n and λ_j^n,*

Sub-problem 1: find $\hat{u}_j^{n+1}$, $\hat{B}_j^{n+1}$, $\hat{p}_j^{n+1}$ and $\hat{\lambda}_j^{n+1}$ satisfying

$$\frac{1}{\Delta t}\hat{u}_j^{n+1} - \frac{\bar{v}^n}{2}\Delta \hat{u}_j^{n+1} + \frac{1}{2}\nabla \hat{p}_j^{n+1} = f_j^{n+1/2} + \frac{1}{\Delta t}u_j^n + v_j'^n \Delta \tilde{u}_j^{n+1/2}$$
$$+ \frac{\bar{v}^n}{2}\Delta u_j^n - \frac{1}{2}\nabla p_j^n, \tag{51a}$$

$$\nabla \cdot \hat{u}_j^{n+1} = 0, \tag{51b}$$

$$\frac{1}{\Delta t}\hat{B}_j^{n+1} - \frac{\bar{\gamma}^n}{2}\Delta \hat{B}_j^{n+1} + \frac{1}{2}\nabla \hat{\lambda}_j^{n+1} = \nabla \times g_j^{n+1/2} + \frac{1}{\Delta t}B_j^n + \frac{\bar{\gamma}^n}{2}\Delta B_j^n \tag{51c}$$
$$+ \gamma_j'^n \Delta \tilde{B}_j^{n+1/2} - \frac{1}{2}\nabla \lambda_j^n,$$

$$\nabla \cdot \hat{B}_j^{n+1} = 0, \tag{51d}$$

Sub-problem 2: find $\breve{u}_j^{n+1}$, $\breve{B}_j^{n+1}$, $\breve{p}_j^{n+1}$ and $\breve{\lambda}_j^{n+1}$ satisfying

$$\frac{1}{\Delta t}\breve{u}_j^{n+1} - \frac{\bar{v}^n}{2}\Delta \breve{u}_j^{n+1} + \frac{1}{2}\nabla \breve{p}_j^{n+1} = s\left(\tilde{B}_j^{n+1/2} \cdot \nabla\right)\tilde{B}_j^{n+1/2} - \left(\tilde{u}_j^{n+1/2} \cdot \nabla\right)\tilde{u}_j^{n+1/2}, \tag{52a}$$

$$\nabla \cdot \breve{u}_j^{n+1} = 0, \tag{52b}$$

$$\frac{1}{\Delta t} \breve{\boldsymbol{B}}_j^{n+1} + \frac{1}{2} \nabla \breve{\lambda}_j^{n+1} - \frac{\bar{\gamma}^n}{2} \Delta \breve{\boldsymbol{B}}_j^{n+1} = \left(\tilde{\boldsymbol{B}}_j^{n+1/2} \cdot \nabla \right) \tilde{\boldsymbol{u}}_j^{n+1/2} - \left(\tilde{\boldsymbol{u}}_j^{n+1/2} \cdot \nabla \right) \tilde{\boldsymbol{B}}_j^{n+1/2},$$
(52c)

$$\nabla \cdot \breve{\boldsymbol{B}}_j^{n+1} = 0.$$
(52d)

Remark 1 For inhomogeneous Dirichlet boundary conditions, let

$$\hat{\boldsymbol{u}}_j^{n+1} = g(x, t^{n+1}), \quad \breve{\boldsymbol{u}}_j^{n+1} = 0, \quad \hat{\boldsymbol{B}}_j^{n+1} = h(x, t^{n+1}), \quad \breve{\boldsymbol{B}}_j^{n+1} = 0 \quad \text{on } \partial\Omega.$$

We use the following approximations,

$$\begin{cases} \bar{\boldsymbol{v}}_j^{n+1} & = \hat{\boldsymbol{v}}_j^{n+1} + \breve{\boldsymbol{v}}_j^{n+1}, & (53) \\ \bar{\boldsymbol{v}}_j^{n+1/2} & = \frac{1}{2}(\bar{\boldsymbol{v}}_j^{n+1} + \boldsymbol{v}^n). & (54) \end{cases}$$

This is a reasonable approximation to use since ξ_j is a second order approximation to 1 and is necessary for our equations to result in a linear update of ξ_j. We then update ξ_j as

$$\xi_j = \frac{\mathscr{F}(R_j^n) + |S_0|\Delta t}{E(\bar{\boldsymbol{u}}_j^{n+1}, \bar{\boldsymbol{B}}_j^{n+1}) + \Delta t \int_\Omega \left(\nu|\nabla \bar{\boldsymbol{u}}_j^{n+1/2}|^2 + s\gamma|\nabla \bar{\boldsymbol{B}}_j^{n+1/2}|^2 \right) d\Omega + \Delta t(|S_0| - S_0)},$$
(55)

where

$$S_0 = \int_\Omega \boldsymbol{f}_j^{n+1/2} \cdot \bar{\boldsymbol{u}}_j^{n+1/2} d\Omega + \int_\Omega s(\nabla \times \boldsymbol{g}_j^{n+1/2}) \cdot \bar{\boldsymbol{B}}_j^{n+1/2} d\Omega + \int_\Gamma B_S \left(\bar{\boldsymbol{u}}_j^{n+1/2}, \bar{\boldsymbol{B}}_j^{n+1/2} \right) d\Gamma.$$
(56)

Notice ξ_j is updated via a linear equation and is very direct. Once we have ξ_j we update

$$R_j^{n+1} = \mathscr{G} \left(\xi_j E(\bar{\boldsymbol{u}}_j^{n+1}, \bar{\boldsymbol{B}}_j^{n+1}) \right)$$
(57)

and proceed to the next timestep iteration. Since ξ_j is a ratio of the SAV to itself, we should expect the result to be close to one. With our ensemble approach in (51)–(52), all J realizations have the same coefficient matrix in each timestep so should be computationally efficient.

Theorem 8 *The scalar ξ_j in (55) and R_j^{n+1} in (57) are guaranteed to be positive at all timesteps.*

Proof By definition (5), $\mathscr{F}(R_j^0) > 0$ so long as $R_j^0 > 0$. It's explained in (3.1) that R_j^0 will be positive. The energy function $E(u, B)$ is always positive and $\int_\Omega \left(\nu|\nabla u|^2 + s\gamma|\nabla B|^2 \right) d\Omega \geq 0$. Since $|S_0| - S_0 \geq 0$, the initially computed ξ_j is ensured positive. Then by induction, ξ_j at any timestep is guaranteed positive.

Once it's ensured $\xi_j > 0$, from the definition (6) we can guarantee R_j^{n+1} in (57) is positive. This completes the proof. □

4.2 BDF2

For Algorithm (2), we develop an efficient implementation with the same approach. Note solving Algorithm (2) is equivalent to the following,

Algorithm 9 *Given $\boldsymbol{u}_j^{n-1}$, $\boldsymbol{u}_j^n$, $\boldsymbol{B}_j^{n-1}$ and $\boldsymbol{B}_j^n$,*

Sub-problem 1: find $\hat{\boldsymbol{u}}_j^{n+1}$, $\hat{\boldsymbol{B}}_j^{n+1}$, $\hat{p}_j^{n+1}$ and $\hat{\lambda}_j^{n+1}$ satisfying

$$\frac{3}{2\Delta t}\hat{\boldsymbol{u}}_j^{n+1} - \bar{\nu}^n \Delta \hat{\boldsymbol{u}}_j^{n+1} + \nabla \hat{p}_j^{n+1} = \boldsymbol{f}_j^{n+1} + \frac{2}{\Delta t}\boldsymbol{u}_j^n - \frac{1}{2\Delta t}\boldsymbol{u}_j^{n-1} + \nu_j'^n \Delta \tilde{\boldsymbol{u}}_j^{n+1}, \tag{58a}$$

$$\nabla \cdot \hat{\boldsymbol{u}}_j^{n+1} = 0, \tag{58b}$$

$$\frac{3}{2\Delta t}\hat{\boldsymbol{B}}_j^{n+1} - \bar{\gamma}^n \Delta \hat{\boldsymbol{B}}_j^{n+1} + \nabla \hat{\lambda}_j^{n+1} = \nabla \times \boldsymbol{g}_j^{n+1} + \frac{2}{\Delta t}\boldsymbol{B}_j^n - \frac{1}{2\Delta t}\boldsymbol{B}_j^{n-1} + \gamma_j'^n \Delta \tilde{\boldsymbol{B}}_j^{n+1}, \tag{58c}$$

$$\nabla \cdot \hat{\boldsymbol{B}}_j^{n+1} = 0, \tag{58d}$$

Sub-problem 2: find $\breve{\boldsymbol{u}}_j^{n+1}$, $\breve{\boldsymbol{B}}_j^{n+1}$, $\breve{p}_j^{n+1}$ and $\breve{\lambda}_j^{n+1}$ satisfying

$$\frac{3}{2\Delta t}\breve{\boldsymbol{u}}_j^{n+1} - \bar{\nu}^n \Delta \breve{\boldsymbol{u}}_j^{n+1} + \nabla \breve{p}_j^{n+1} = s\left(\tilde{\boldsymbol{B}}_j^{n+1} \cdot \nabla\right)\tilde{\boldsymbol{B}}_j^{n+1} - \left(\tilde{\boldsymbol{u}}_j^{n+1} \cdot \nabla\right)\tilde{\boldsymbol{u}}_j^{n+1}, \tag{59a}$$

$$\nabla \cdot \hat{\boldsymbol{u}}_j^{n+1} = 0, \tag{59b}$$

$$\frac{3}{2\Delta t}\breve{\boldsymbol{B}}_j^{n+1} - \bar{\gamma}^n \Delta \breve{\boldsymbol{B}}_j^{n+1} + \nabla \breve{\lambda}_j^{n+1} = \left(\tilde{\boldsymbol{B}}_j^{n+1} \cdot \nabla\right)\tilde{\boldsymbol{u}}_j^{n+1} - \left(\tilde{\boldsymbol{u}}_j^{n+1} \cdot \nabla\right)\tilde{\boldsymbol{B}}_j^{n+1}, \tag{59c}$$

$$\nabla \cdot \hat{\boldsymbol{B}}_j^{n+1} = 0. \tag{59d}$$

We use the following approximations,

$$\begin{cases} \bar{\boldsymbol{v}}_j^{n+1} & = \hat{\boldsymbol{v}}_j^{n+1} + \breve{\boldsymbol{v}}_j^{n+1}, & (60) \\ \bar{\boldsymbol{v}}_j^{n+3/2} & = \frac{3}{2}\bar{\boldsymbol{v}}_j^{n+1} - \frac{1}{2}\boldsymbol{v}^n, & (61) \end{cases}$$

again noting ξ_j is a second order approximation to 1. We update ξ_j as

$$\xi_j = \frac{\mathscr{F}(\overset{*}{R}_j^{n+1/2}) + |S_0|\Delta t}{E(\bar{\boldsymbol{u}}_j^{n+3/2}, \bar{\boldsymbol{B}}_j^{n+3/2}) + \Delta t \int_\Omega \left(\nu|\nabla\bar{\boldsymbol{u}}_j^{n+1}|^2 + s\gamma|\nabla\bar{\boldsymbol{B}}_j^{n+1}|^2\right)d\Omega + \Delta t(|S_0| - S_0)}, \tag{62}$$

where

$$S_0 = \int_\Omega \boldsymbol{f}_j^{n+1} \cdot \bar{\boldsymbol{u}}_j^{n+1}d\Omega + \int_\Omega s\left(\nabla \times \boldsymbol{g}_j^{n+1}\right) \cdot \bar{\boldsymbol{B}}_j^{n+1}d\Omega + \int_\Gamma B_S\left(\bar{\boldsymbol{u}}_j^{n+1}, \bar{\boldsymbol{B}}_j^{n+1}\right)d\Gamma.$$

Once we have ξ_j we update R_j^{n+1} as follows:

$$\begin{cases} \overset{*}{R}_j^{n+3/2} & = \mathscr{G}\left(\xi_j E\left(\bar{\boldsymbol{u}}_j^{n+3/2}, \bar{\boldsymbol{B}}_j^{n+3/2}\right)\right), & (63) \\ R_j^{n+1} & = \frac{2}{3}\overset{*}{R}_j^{n+3/2} + \frac{1}{3}R_j^n. & (64) \end{cases}$$

and proceed to the next timestep iteration.

Theorem 10 *The scalar ξ_j in (62) and R_j^{n+1} in (64) are guaranteed to be positive at all timesteps if the approximation $\overset{*}{R}_j^{1/2} > 0$.*

Proof Again by definition (5), $\mathscr{F}(\overset{*}{R}_j^{1/2}) > 0$ so long as approximation $\overset{*}{R}_j^{1/2} > 0$. The argument for positivity of ξ_j proceeds identically to that made in the proof of Theorem (8).

Once it's ensured $\xi_j > 0$, again from definition (6) we can guarantee $\overset{*}{R}_j^{n+3/2}$ in (63) is positive. It's also guaranteed R_j^0 is positive from the previously stated point that it would be initialized as $\mathscr{G}(E(\boldsymbol{u}_j^0(x), \boldsymbol{B}_j^0(x)))$. Thus we conclude R_j^{n+1} in (64) remains positive. This completes the proof. □

5 Numerical Tests

This section will present numerical results for Algorithms (3) and (4) to demonstrate the expected convergence rates and the stability proven previously. We set $\mathscr{F}(\chi) = \chi^2$ and the corresponding $\mathscr{G}(\chi) = \sqrt{\chi}$ in every experiment. Throughout these tests we'll use the finite element triplet $(P^2 - P^1 - P^2)$, and the finite element software package FEniCS [42].

5.1 Convergence Test

To verify the expected convergence rates, we will use a variation of the test problem in [43]. Take the time interval $0 \le t \le 1$ and domain $\Omega = [0, 1]^2$. Define the true solution (u, p, B) as

$$\begin{cases} u_\epsilon = \left(y^5 + t^2, x^5 + t^2\right)(1 + \epsilon), \\ p_\epsilon = 10(2x - 1)(2y - 1)(1 + t^2)(1 + \epsilon), \\ B_\epsilon = \left(\sin(\pi y) + t^2, \sin(\pi x) + t^2\right)(1 + \epsilon), \end{cases}$$

where ϵ is a given perturbation. For this problem we will consider two perturbations $\epsilon_1 = 10^{-1}$ and $\epsilon_2 = -10^{-1}$. The kinematic viscosity and magnetic resistivity are defined as $\nu_\epsilon = 0.5 \cdot (1 + \epsilon)$ and $\gamma_\epsilon = 0.5 \cdot (1 + \epsilon)$. The source terms and initial conditions correspond with the exact solution for the given perturbation. For each algorithm we initialize u_j, B_j, p_j or λ_j using the exact solution. The results are displayed in Tables 1, 2, 3, 4, 5, 6, 7 and 8 both with regularization and without ($\alpha = \alpha_M = 0$). Under this test, we indeed observe second order convergence with and without regularization. In this particular test on a short time interval, we also observe the algorithm with regularization achieves relatively similar accuracy to the algorithm without.

5.2 Efficiency Test

In this experiment we repeat the numerical methods used above with the same problem, except we set $\nu_\epsilon = 1.0 \cdot (1 + \epsilon)$, $\gamma_\epsilon = 0.2 \cdot (1 + \epsilon)$ and analyze 11 perturbations $\epsilon_i = 10^{-1} - 0.009 * i$, $i = 0, \ldots, 10$. We compare the performance speed and accuracy of Algorithms (3) and (4) with the corresponding nonensemble GPAV methods, where no ensemble mean is used and the linear systems for each perturbation are solved in serial. To do this, we list the CPU runtime in seconds and error norm of the average of all 11 velocities and magnetic fields, labeled as $\bar{u}^n$ and $\bar{B}^n$, for each computation. As can be seen in the Tables 9, 10, 11 and 12 below, the second order ensemble methods obtain the same accuracy as the nonensemble trials, while requiring significantly less runtime (Tables 13 and 14).

Table 1 Crank–Nicolson error and convergence rates for the first ensemble member in u_h and ∇u_h

h	Δt	$\|u_1 - u_{1,h}\|_{\infty,0_{rel}}$	Rate	$\|\nabla u_1 - \nabla u_{1,h}\|_{2,0_{rel}}$	Rate
1/10	1/8	9.191 e–4	–	4.985 e–3	–
1/20	1/16	2.088 e–4	2.138	1.399 e–3	1.834
1/40	1/32	4.810 e–5	2.118	3.679 e–4	1.927
1/80	1/64	1.154 e–5	2.060	9.422 e–5	1.965
1/160	1/128	2.889 e–6	1.998	2.384 e–5	1.983
Reg with $\alpha = \alpha_M = 0.5$					
1/10	1/8	3.912 e–4	–	4.741 e–3	–
1/20	1/16	6.032 e–5	2.697	1.355 e–3	1.807
1/40	1/32	9.532 e–6	2.662	3.579 e–4	1.920
1/80	1/64	2.208 e–6	2.110	9.179 e–5	1.963

Table 2 Crank–Nicolson error and convergence rates for the first ensemble member in B_h and ∇B_h

h	Δt	$\|B_1 - B_{1,h}\|_{\infty,0_{rel}}$	Rate	$\|\nabla B_1 - \nabla B_{1,h}\|_{2,0_{rel}}$	Rate
1/10	1/8	2.566 e–4	–	3.013 e-3	–
1/20	1/16	5.0568 e–5	2.343	8.451 e–4	1.834
1/40	1/32	1.150 e–5	2.136	2.223 e–4	1.927
1/80	1/64	2.746 e–6	2.067	5.694 e–5	1.965
1/160	1/128	6.869 e–7	1.999	1.440 e–5	1.983
Reg with $\alpha = \alpha_M = 0.5$					
1/10	1/8	1.512 e–4	–	2.909 e–3	–
1/20	1/16	2.138 e–5	2.822	8.298 e–4	1.810
1/40	1/32	3.082 e–6	2.795	2.191 e–4	1.921
1/80	1/64	6.830 e–7	2.174	5.619 e–5	1.964

Table 3 Crank–Nicolson error and convergence rates for the second ensemble member in u_h and ∇u_h

h	Δt	$\|u_2 - u_{2,h}\|_{\infty,0_{rel}}$	Rate	$\|\nabla u_2 - \nabla u_{2,h}\|_{2,0_{rel}}$	Rate
1/10	1/8	2.020 e–3	–	5.498 e–3	–
1/20	1/16	4.897 e–4	2.045	1.433 e–3	1.940
1/40	1/32	9.342 e–5	2.390	3.701 e–4	1.953
1/80	1/64	1.560 e–5	2.582	9.440 e–5	1.971
1/160	1/128	2.923 e–6	2.416	2.385 e–5	1.985
Reg with $\alpha = \alpha_M = 0.5$					
1/10	1/8	4.070 e–4	–	4.753 e–3	–
1/20	1/16	6.277 e–5	2.697	1.357 e–3	1.809
1/40	1/32	1.134 e–5	2.469	3.584 e–4	1.921
1/80	1/64	2.649 e–6	2.097	9.190 e–5	1.964

Table 4 Crank–Nicolson error and convergence rates for the second ensemble member in B_h and ∇B_h

h	Δt	$\|B_2 - B_{2,h}\|_{\infty,0_{rel}}$	Rate	$\|\nabla B_2 - \nabla B_{2,h}\|_{2,0_{rel}}$	Rate
1/10	1/8	7.455 e–4	–	3.376 e–3	–
1/20	1/16	1.666 e–4	2.162	8.700 e–4	1.956
1/40	1/32	3.097 e–5	2.427	2.239 e–4	1.958
1/80	1/64	5.113 e–6	2.598	5.706 e–5	1.973
1/160	1/128	7.772 e–7	2.718	1.442 e–5	1.985
Reg with $\alpha = \alpha_M = 0.5$					
1/10	1/8	1.567 e–4	–	2.915 e–3	–
1/20	1/16	2.222 e–5	2.818	8.308 e–4	1.811
1/40	1/32	3.664 e–6	2.600	2.193 e–4	1.922
1/80	1/64	8.188 e–7	2.162	5.622 e–5	1.964

Table 5 BDF2 error and convergence rates for the first ensemble member in u_h and ∇u_h

h	Δt	$\|u_1 - u_{1,h}\|_{\infty,0_{rel}}$	Rate	$\|\nabla u_1 - \nabla u_{1,h}\|_{2,0_{rel}}$	Rate
1/10	1/8	7.413 e–4	–	5.804 e–3	–
1/20	1/16	1.891 e–4	1.971	1.495 e–3	1.957
1/40	1/32	4.790 e–5	1.981	3.793 e–4	1.978
1/80	1/64	1.183 e–5	2.018	9.557 e–5	1.989
1/160	1/128	2.944 e–6	2.006	2.399 e–5	1.994
Reg with $\alpha = \alpha_M = 0.5$					
1/10	1/8	4.528 e–4	–	5.601 e–3	–
1/20	1/16	6.215 e–5	2.865	1.453 e–3	1.947
1/40	1/32	7.946 e–6	2.968	3.694 e–4	1.976
1/80	1/64	1.339 e–6	2.570	9.310 e–5	1.988

Table 6 BDF2 error and convergence rates for the first ensemble member in B_h and ∇B_h

h	Δt	$\|B_1 - B_{1,h}\|_{\infty,0_{rel}}$	Rate	$\|\nabla B_1 - \nabla B_{1,h}\|_{2,0_{rel}}$	Rate
1/10	1/8	1.868 e–4	–	3.502 e–3	–
1/20	1/16	3.792 e–5	2.301	9.005 e–4	1.960
1/40	1/32	9.133 e–6	2.054	2.285 e–4	1.979
1/80	1/64	2.300 e–6	1.990	5.756 e–5	1.989
1/160	1/128	5.816 e–7	1.983	1.445 e–5	1.994
Reg with $\alpha = \alpha_M = 0.5$					
1/10	1/8	1.649 e–4	–	3.438 e–3	–
1/20	1/16	2.185 e–5	2.916	8.904 e–4	1.949
1/40	1/32	2.772 e–6	2.978	2.263 e–4	1.976
1/80	1/64	4.182 e–7	2.729	5.705 e–5	1.988

Table 7 BDF2 error and convergence rates for the second ensemble member in u_h and ∇u_h

h	Δt	$\|u_2 - u_{2,h}\|_{\infty,0_{rel}}$	Rate	$\|\nabla u_2 - \nabla u_{2,h}\|_{2,0_{rel}}$	Rate
1/10	1/8	7.762 e–4	–	5.806 e–3	–
1/20	1/16	1.880 e–4	2.045	1.495 e–3	1.957
1/40	1/32	4.699 e–5	2.001	3.795 e–4	1.978
1/80	1/64	1.186 e–5	1.987	9.561 e–5	1.989
1/160	1/128	2.964 e–6	2.001	2.400 e–5	1.994
Reg with $\alpha = \alpha_M = 0.5$					
1/10	1/8	4.531 e–4	–	5.603 e–3	–
1/20	1/16	6.218 e–5	2.865	1.453 e–3	1.947
1/40	1/32	7.964 e–6	2.965	3.695 e–4	1.976
1/80	1/64	1.547 e–6	2.364	9.314 e–5	1.988

Table 8 BDF2 error and convergence rates for the second ensemble member in B_h and ∇B_h

h	Δt	$\|B_2 - B_{2,h}\|_{\infty,0_{rel}}$	Rate	$\|\nabla B_2 - \nabla B_{2,h}\|_{2,0_{rel}}$	Rate
1/10	1/8	1.918 e–4	–	3.505 e–3	–
1/20	1/16	3.930 e–5	2.287	9.013 e–4	1.960
1/40	1/32	9.605 e–6	2.033	2.287 e–4	1.979
1/80	1/64	2.425 e–6	1.986	5.761 e–5	1.989
1/160	1/128	6.129 e–7	1.984	1.446 e–5	1.994
Reg with $\alpha = \alpha_M = 0.5$					
1/10	1/8	1.649 e–3	–	3.439 e–3	–
1/20	1/16	2.185 e–4	2.916	8.906 e–4	1.949
1/40	1/32	2.772 e–4	2.978	2.264 e–4	1.976
1/80	1/64	4.880 e–5	2.506	5.706 e–5	1.988

Table 9 Error and CPU time for computing $\bar{u}_h$ and $\bar{B}_h$ with Algorithm 3

h	Δt	$\|\bar{u} - \bar{u}_{en,h}\|_{\infty,0_{rel}}$	$\|\bar{B} - \bar{B}_{en,h}\|_{\infty,0_{rel}}$	CPU time (s)
1/5	1/40	3.099 e–3	1.220 e–3	2.117 e+0
1/10	1/80	4.782 e–4	1.716 e–4	7.622 e+0
1/20	1/160	6.294 e–5	2.218 e–5	3.911 e+1
1/40	1/320	7.968 e–6	2.802 e–6	2.905 e+2
1/80	1/640	1.005 e–6	4.450 e–7	2.181 e+3

Table 10 Error and CPU time for computing $\bar{u}_h$ and $\bar{B}_h$ with nonensemble CN algorithm

h	Δt	$\|\bar{u} - \bar{u}_{en,h}\|_{\infty,0_{rel}}$	$\|\bar{B} - \bar{B}_{en,h}\|_{\infty,0_{rel}}$	CPU time (s)
1/10	1/80	4.783 e–4	1.718 e–4	1.694 e+1
1/20	1/160	6.294 e–5	2.219 e–5	1.144 e+2
1/40	1/320	7.968 e–6	2.802 e–6	8.362 e+2
1/80	1/640	1.004 e–6	7.730 e–7	6.895 e+3

Table 11 Error and CPU time for computing $\bar{u}_h$ and $\bar{B}_h$ with Algorithm 4

h	Δt	$\|\bar{u} - \bar{u}_{en,h}\|_{\infty,0_{rel}}$	$\|\bar{B} - \bar{B}_{en,h}\|_{\infty,0_{rel}}$	CPU time (s)
1/5	1/40	3.609 e–3	1.331 e–3	2.768 e+0
1/10	1/80	4.961 e–4	1.750 e–4	8.432 e+0
1/20	1/160	6.348 e–5	2.219 e–5	3.844 e+1
1/40	1/320	7.982 e–6	2.785 e–6	2.760 e+2
1/80	1/640	1.006 e–6	3.546 e–7	2.267 e+3

Table 12 Error and CPU time for computing $\bar{u}_h$ and $\bar{B}_h$ with nonensemble BDF2 algorith

h	Δt	$\|\bar{u} - \bar{u}_{en,h}\|_{\infty,0_{rel}}$	$\|\bar{B} - \bar{B}_{en,h}\|_{\infty,0_{rel}}$	CPU time (s)
1/10	1/80	4.962 e–4	1.750 e–4	1.674 e+1
1/20	1/160	6.348 e–5	2.219 e–5	1.152 e+2
1/40	1/320	7.982 e–6	2.785 e–6	8.233 e+2
1/80	1/640	1.006 e–6	3.549 e–7	6.720 e+3

5.3 Stability

Here we analyze the stability of the second order ensemble methods. For the test problem, we will exclude external energy and body forces so that in observation if the method is stable, the system energy should decay to zero as time passes. We also use the initial conditions,

$$\begin{cases} u_\epsilon^0 = (x^2(x-1)^2 y(y-1)(2y-1), -y^2(y-1)^2 x(x-1)(2x-1))(1+\epsilon), \\ p_\epsilon^0 = 0, \\ B_\epsilon^0 = (\sin(\pi x)\cos(\pi y), -\sin(\pi y)\cos(\pi x))(1+\epsilon). \end{cases}$$

We'll consider an ensemble of two perturbations, $\epsilon = 10^{-1}$ and $\epsilon = -10^{-1}$. We fix the coupling term $s = 1$ and choose two different sets of viscosity and magnetic viscosity to test, $\nu = \gamma = 0.1$ and $\nu = \gamma = 0.02$. The mesh discretization is fixed at $h = 1/50$ and several time steps are employed, with final time $T = 5$.
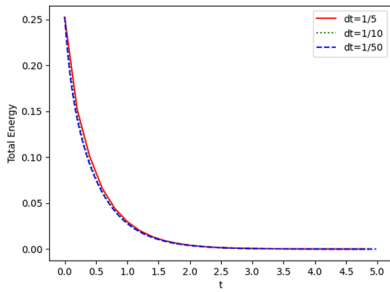
(a) Decay of total system energy to $T = 5$ for Algorithm (3) with $\nu = \gamma = 0.1$.
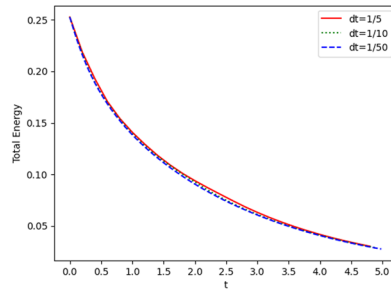
(b) Decay of total system energy to $T = 5$ for Algorithm (3) with $\nu = \gamma = 0.02$.
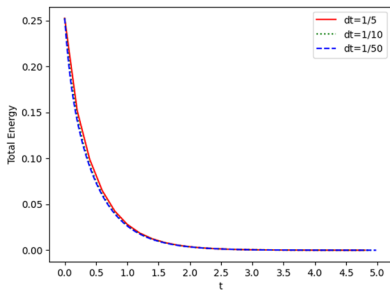
(c) Decay of total system energy to $T = 5$ for Algorithm (4) with $\nu = \gamma = 0.1$.
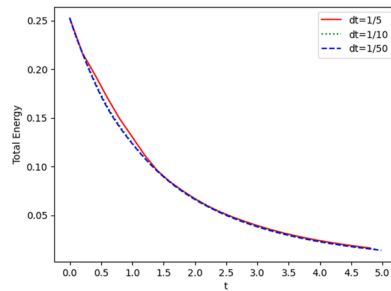
(d) Decay of total system energy to $T = 5$ for Algorithm (4) with $\nu = \gamma = 0.02$.

5.4 Chamber Flow

In this numerical test, we consider a channel flow in a rectangular domain of length 2.2 units and height 0.41, with a cylinder of radius 0.05 centered at $(0.2, 0.2)$, in the presence of a magnetic field. On the walls and around the cylinder, a no-slip boundary condition is applied for velocity while magnetic field is kept constant as $B =< 0, 0.1 >^T$. We set the inflow and outflow conditions equal, choosing $u =< 6y(0.41 - y)/0.41^2 \sin(\pi t/16.0), 0 >^T$ and $B =< 0, 0.1 >^T$. The coupling term is set to $s = 0.01$ and for all realizations we fix $\gamma = 0.1$ then consider two cases, $\nu = 1/50$ and $\nu = 1/1000$.

We'll use an ensemble of two different solutions with the initial and boundary conditions perturbed by multiplicative factors of $(1 \pm \epsilon)$. We simulate the flow with Algorithms (3) and (4) till final time $T = 8.8$ with a mesh discretization fixed at $h = 1/100$. We set $\alpha = \alpha_M = 0$ such that these tests are performed without the regularization terms involved. In order to maintain accurate results up unto $T = 8.8$, we find it necessary to choose a time step of roughly $\Delta t = 1/1000$ when $\nu = 1/50$ and $\Delta t = 1/2000$ when $\nu = 1/1000$. The solutions under each perturbation for velocity are shown in Figs. 1, 2, 3 and 4 and for magnetic field in Figs. 7, 8, 9 and 10. We also provide results for no perturbation, that is, $\epsilon = 0$. This is for comparison as we expect the ensemble solutions to converge to the unperturbed results as $\epsilon \to 0$ (Figs. 5 and 6).
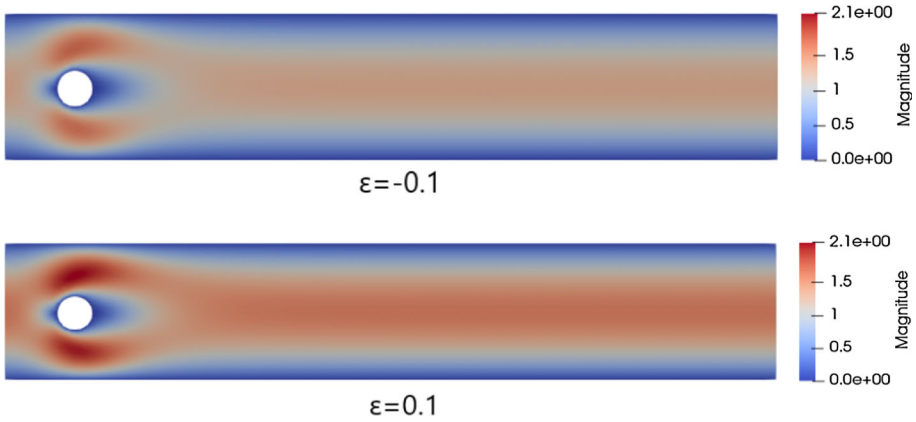
Fig. 1 Ensemble solutions for velocity at time $T = 8.8$ for Algorithm (3) with $\nu = 0.02$, $\gamma = 0.1$ and $\Delta t = 0.001$
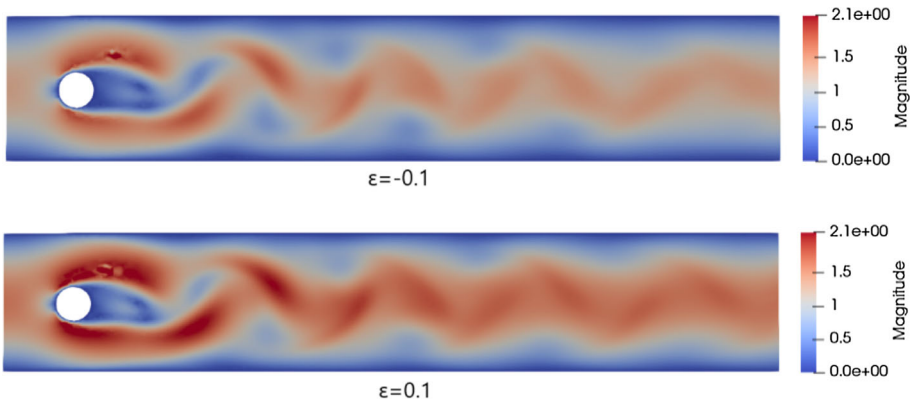
Fig. 2 Ensemble solutions for velocity at time $T = 8.8$ for Algorithm (3) with $\nu = 0.001$, $\gamma = 0.1$ and $\Delta t = 0.0005$
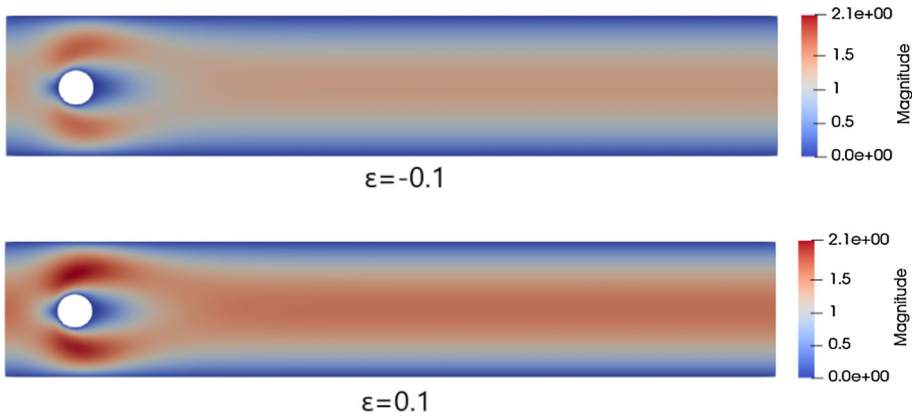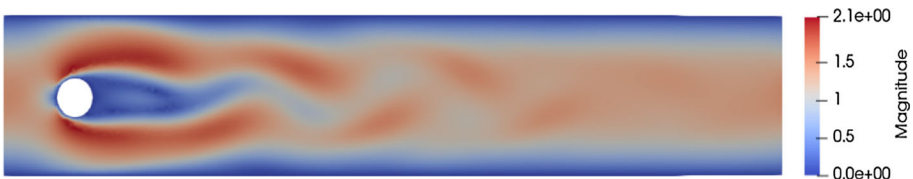

Fig. 3 Ensemble solutions for velocity at time $T = 8.8$ for Algorithm (4) with $\nu = 0.02$, $\gamma = 0.1$ and $\Delta t = 0.001$
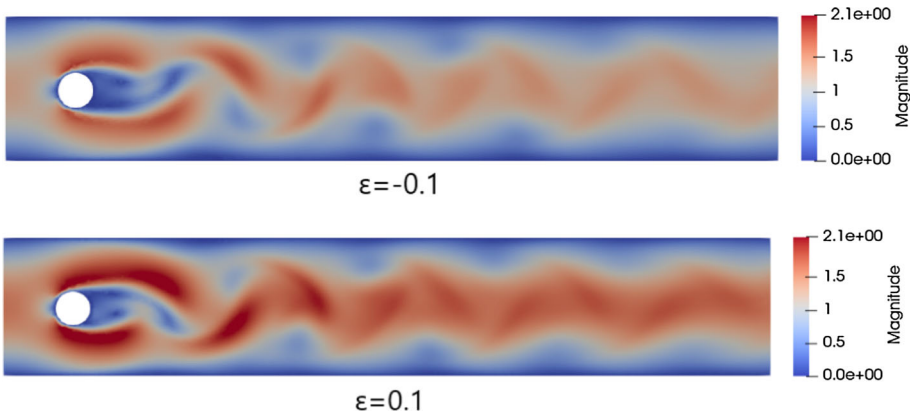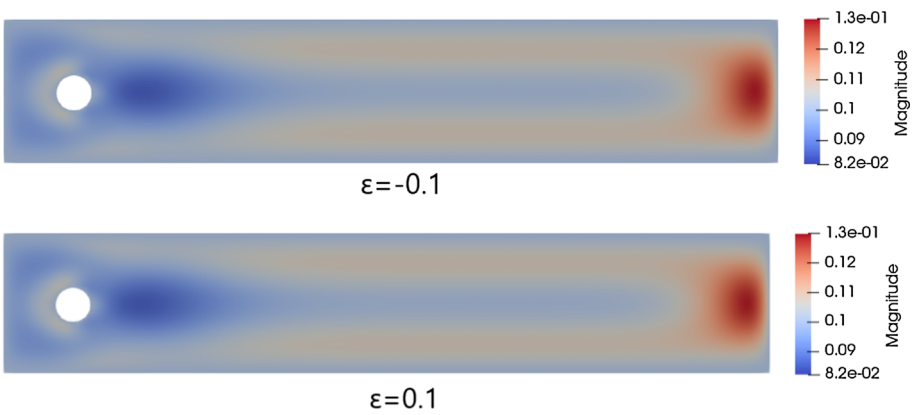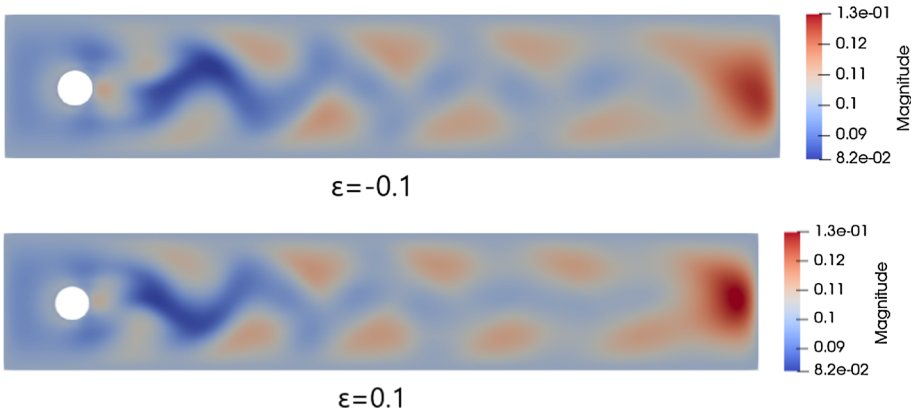
Fig. 4 Ensemble solutions for velocity at time $T = 8.8$ for Algorithm (4) with $\nu = 0.001$, $\gamma = 0.1$ and $\Delta t = 0.0005$
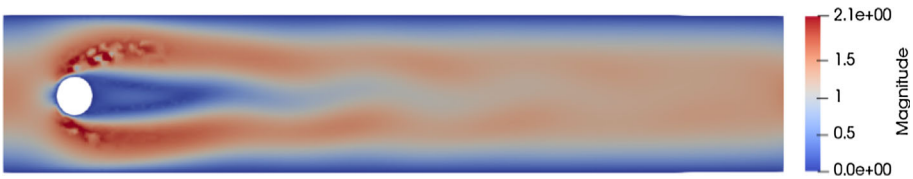
Fig. 5 Algorithm (3) solution when $\epsilon = 0$ for velocity at time $T = 8.8$ with $\nu = 0.001$, $\gamma = 0.1$ and $\Delta t = 0.001$

Fig. 6 Algorithm (4) solution when $\epsilon = 0$ for velocity at time $T = 8.8$ with $\nu = 0.001$, $\gamma = 0.1$ and $\Delta t = 0.001$

Fig. 7 Ensemble solutions for magnetic field at time $T = 8.8$ for Algorithm (3) with $\nu = 0.02$, $\gamma = 0.1$ and $\Delta t = 0.001$
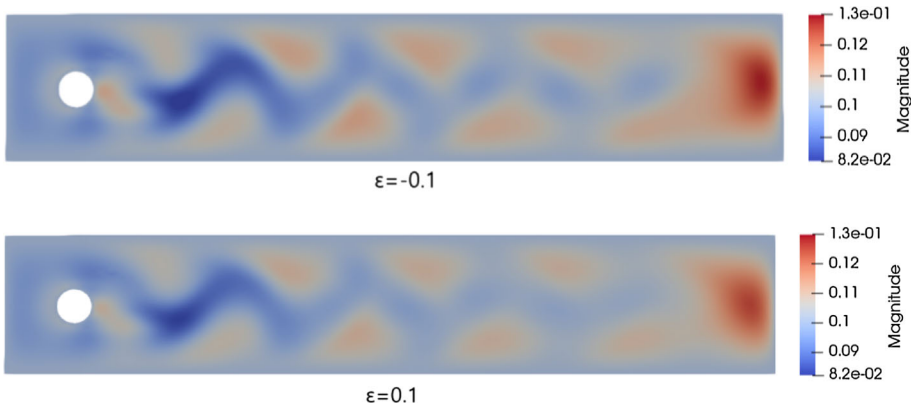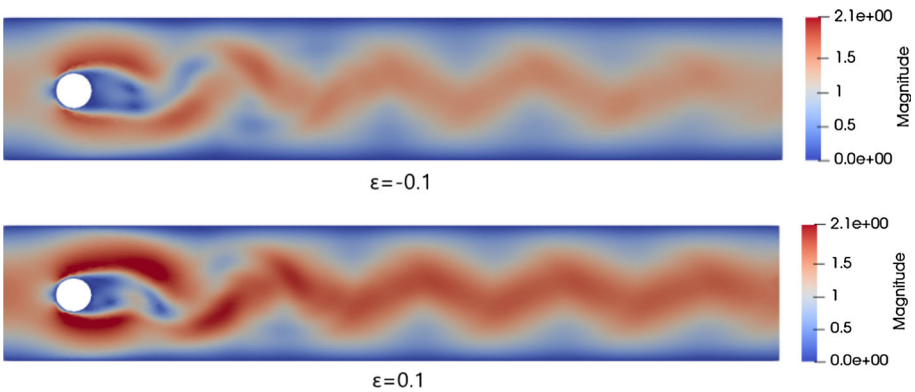
Fig. 8 Ensemble solutions for magnetic field at time $T = 8.8$ for Algorithm (3) with $\nu = 0.001$, $\gamma = 0.1$ and $\Delta t = 0.0005$
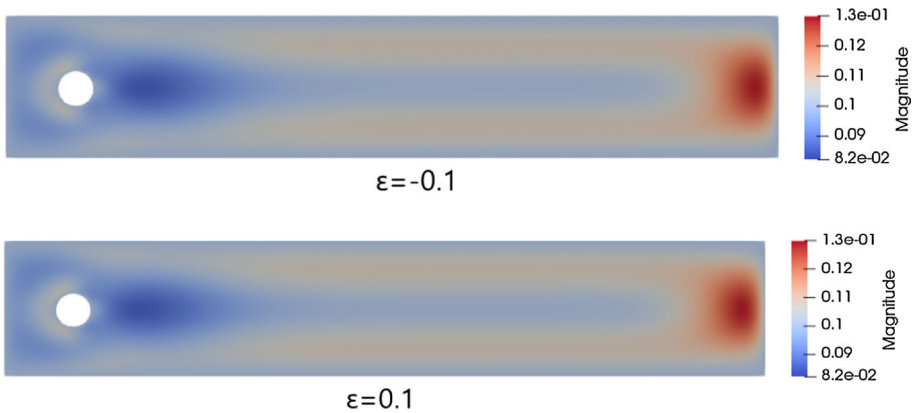
Fig. 9 Ensemble solutions for magnetic field at time $T = 8.8$ for Algorithm (4) with $\nu = 0.02$, $\gamma = 0.1$ and $\Delta t = 0.001$

5.5 Chamber Flow with Regularization

Here we present the same chamber flow problem implementing Algorithms (3) and (4) with nonzero regularization coefficients. We choose $\alpha = \nu$ and $\alpha_M = \gamma$ in each test. We're able to achieve similar accuracy to the previous section with coarser time step. The following numerical results are achieved (Figs. 11, 12, 13, 14 15, and 16):

5.6 Accuracy Comparison

In this section we present a comparison test between the errors of the scheme with and without the regularization terms introduced in Sect. 5.5. We use the same test as in Sect. 5.1, except this time we set $\nu = 1.0$ and $\gamma = 0.2$. We choose two perturbations of $\epsilon = 0.1$ and $\epsilon = 0.2$, with final time $T = 2.5$. This time we use only the L^2 error norm of the result at final time T.

Fig. 10 Ensemble solutions for magnetic field at time $T = 8.8$ for Algorithm (4) with $\nu = 0.001$, $\gamma = 0.1$ and $\Delta t = 0.0005$
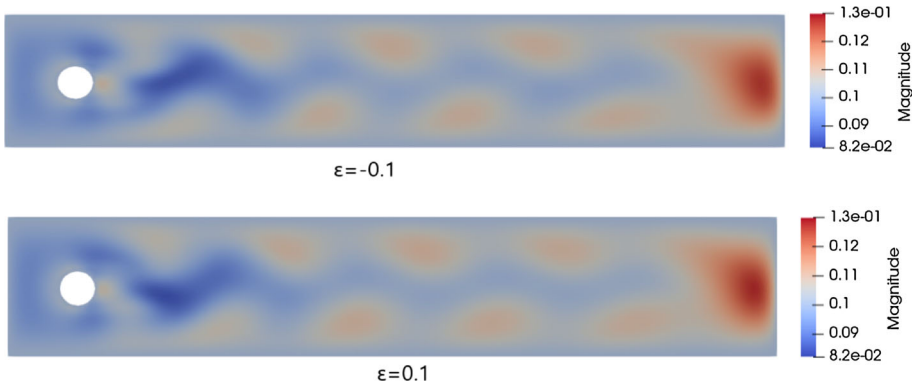

Fig. 11 Algorithm (3) solution when $\epsilon = 0$ for magnetic field at time $T = 8.8$ with $\nu = 0.001$, $\gamma = 0.1$ and $\Delta t = 0.001$
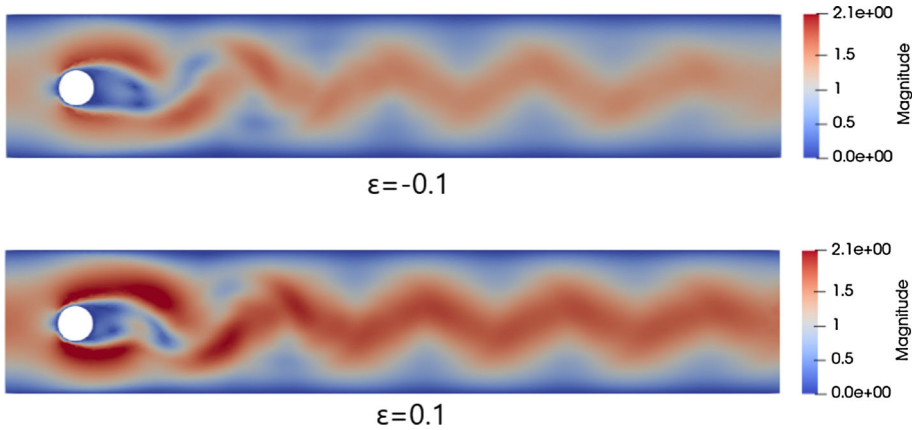

Fig. 12 Algorithm (4) solution when $\epsilon = 0$ for magnetic field at time $T = 8.8$ with $\nu = 0.001$, $\gamma = 0.1$ and $\Delta t = 0.001$
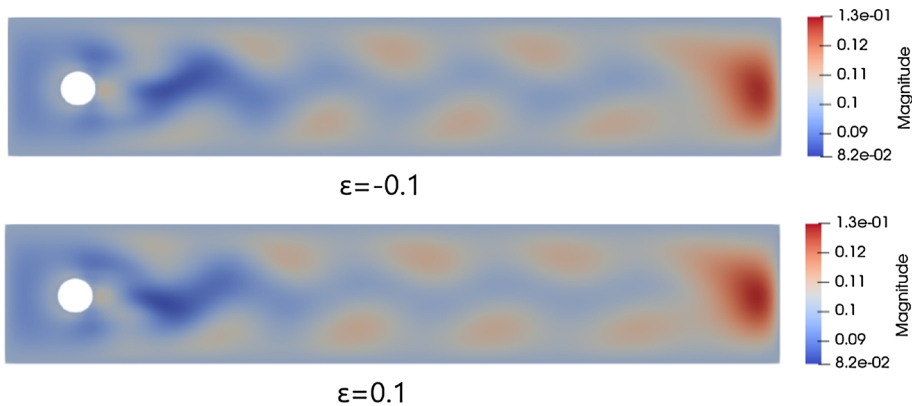

Fig. 13 Ensemble solutions for velocity at time $T = 8.8$ for Algorithm (3) with regularization and $\nu = 0.001$, $\gamma = 0.1$ and $\Delta t = 0.001$

Fig. 14 Ensemble solutions for magnetic field at time $T = 8.8$ for Algorithm (3) with regularization and $\nu = 0.001$, $\gamma = 0.1$ and $\Delta t = 0.001$

Fig. 15 Ensemble solutions for velocity at time $T = 8.8$ for Algorithm (4) with regularization and $\nu = 0.001$, $\gamma = 0.1$ and $\Delta t = 0.001$

Fig. 16 Ensemble solutions for magnetic field at time $T = 8.8$ for Algorithm (4) with regularization and $\nu = 0.001$, $\gamma = 0.1$ and $\Delta t = 0.001$

Table 13 Error for the first ensemble member in u_h

h	Δt	SAV-CN	SAV-BDF2	Stab-SAV-CN	Stab-SAV-BDF2
1/100	1/8	1.398 e–2	3.789 e–2	6.485 e–6	1.823 e–5
1/100	1/16	8.242 e–2	6.229 e–2	3.467 e–6	4.143 e–6
1/100	1/32	3.369 e–2	3.664 e–2	1.907 e–6	9.296 e–7
1/100	1/64	2.230 e–2	9.960 e–3	7.120 e–7	1.902 e–7
1/100	1/128	4.517 e–2	2.383 e–3	1.093 e–6	5.102 e–8

Table 14 Error for the first ensemble member in B_h

h	Δt	SAV-CN	SAV-BDF2	Stab-SAV-CN	Stab-SAV-BDF2
1/100	1/8	5.219 e–2	1.312 e–1	3.074 e–5	6.940 e–5
1/100	1/16	2.644 e–1	1.962 e–1	1.647 e–5	1.592 e–5
1/100	1/32	7.231 e–2	7.033 e–2	9.188 e–6	3.429 e–6
1/100	1/64	6.947 e–2	2.400 e–2	3.318 e–6	6.148 e–7
1/100	1/128	1.061 e–1	8.650 e–3	5.619 e–6	1.390 e–7

For the stabilization coefficients α and α_M, we set them equal to the viscosity and magnetic resistivity correspondingly.

Data Availability Enquiries about data availability should be directed to the authors.

Declarations

Conflict of interest The authors have not disclosed any competing interests.

References

1. Mohebujjaman, M., Rebholz, L.G.: An efficient algorithm for computation of MHD flow ensembles. Comput. Methods Appl. Math. **17**(1), 121–137 (2017). https://doi.org/10.1515/cmam-2016-0033
2. Wei, D., Zhang, Z.: Global well-posedness of the MHD equations in a homogeneous magnetic field. Anal. PDE **10**(6), 1361–1406 (2017). https://doi.org/10.2140/apde.2017.10.1361
3. Trenchea, C.: Unconditional stability of a partitioned IMEX method for magnetohydrodynamic flows. Appl. Math. Lett. **27**, 97–100 (2014). https://doi.org/10.1016/j.aml.2013.06.017
4. Mohebujjaman, M., Wang, H., Rebholz, L.G., Mahbub, M.A.A.: An efficient algorithm for simulating ensembles of parameterized MHD flow problems (2021). arXiv:2108.05110
5. Jiang, N., Layton, W.: An algorithm for fast calculation of flow ensembles. Int. J. Uncertain. Quantif. **4**(4), 273–301 (2014). https://doi.org/10.1615/Int.J.UncertaintyQuantification.2014007691
6. Jiang, N., Layton, W.: Numerical analysis of two ensemble eddy viscosity numerical regularizations of fluid motion. Numer. Methods Partial Differ. Equ. **31**(3), 630–651 (2015). https://doi.org/10.1002/num.21908

7. Jiang, N.: A higher order ensemble simulation algorithm for fluid flows. J. Sci. Comput. **64**(1), 264–288 (2015). https://doi.org/10.1007/s10915-014-9932-z

8. Jiang, N.: A second-order ensemble method based on a blended backward differentiation formula timestepping scheme for time-dependent Navier–Stokes equations. Numer. Methods Partial Differ. Equ. **33**(1), 34–61 (2017). https://doi.org/10.1002/num.22070

9. Gunzburger, M., Jiang, N., Schneier, M.: An ensemble-proper orthogonal decomposition method for the nonstationary Navier–Stokes equations. SIAM J. Numer. Anal. **55**(1), 286–304 (2017). https://doi.org/10.1137/16M1056444

10. Fiordilino, J.A.: A second order ensemble time stepping algorithm for natural convection. SIAM J. Numer. Anal. **56**(2), 816–837 (2018). https://doi.org/10.1137/17M1135104

11. Jiang, N.: A pressure-correction ensemble scheme for computing evolutionary Boussinesq equations. J. Sci. Comput. **80**(1), 315–350 (2019). https://doi.org/10.1007/s10915-019-00939-w

12. Gunzburger, M., Jiang, N., Wang, Z.: An efficient algorithm for simulating ensembles of parameterized flow problems. IMA J. Numer. Anal. **39**(3), 1180–1205 (2019). https://doi.org/10.1093/imanum/dry029

13. Jiang, N., Qiu, C.: An efficient ensemble algorithm for numerical approximation of stochastic Stokes-Darcy equations. Comput. Methods Appl. Mech. Eng. **343**, 249–275 (2019). https://doi.org/10.1016/j.cma.2018.08.020

14. Jiang, N., Li, Y., Yang, H.: An artificial compressibility Crank–Nicolson leap-frog method for the Stokes-Darcy model and application in ensemble simulations. SIAM J. Numer. Anal. **59**(1), 401–428 (2021). https://doi.org/10.1137/20M1321644

15. Jiang, N., Schneier, M.: An efficient, partitioned ensemble algorithm for simulating ensembles of evolutionary MHD flows at low magnetic Reynolds number. Numer. Methods Partial Differ. Equ. **34**(6), 2129–2152 (2018). https://doi.org/10.1002/num.22281

16. Carter, J., Jiang, N.: Numerical analysis of a second order ensemble method for evolutionary magnetohydrodynamics equations at small magnetic Reynolds number. Numer. Methods Partial Differ. Equ. (2022). https://doi.org/10.1002/num.22843

17. Elsasser, W.M.: The hydromagnetic equations. Phys. Rev. **79**, 183–183 (1950). https://doi.org/10.1103/PhysRev.79.183

18. Guillén-González, F., Tierra, G.: On linear schemes for a Cahn–Hilliard diffuse interface model. J. Comput. Phys. **234**, 140–171 (2013). https://doi.org/10.1016/j.jcp.2012.09.020

19. Yang, X., Zhao, J., Wang, Q.: Numerical approximations for the molecular beam epitaxial growth model based on the invariant energy quadratization method. J. Comput. Phys. **333**, 104–127 (2017). https://doi.org/10.1016/j.jcp.2016.12.025

20. Yang, X., Ju, L.: Linear and unconditionally energy stable schemes for the binary fluid-surfactant phase field model. Comput. Methods Appl. Mech. Eng. **318**, 1005–1029 (2017). https://doi.org/10.1016/j.cma.2017.02.011

21. Gong, Y., Zhao, J., Wang, Q.: Arbitrarily high-order linear energy stable schemes for gradient flow models. J. Comput. Phys. **419**, 109610–20 (2020). https://doi.org/10.1016/j.jcp.2020.109610

22. Shen, J., Xu, J., Yang, J.: The scalar auxiliary variable (SAV) approach for gradient flows. J. Comput. Phys. **353**, 407–416 (2018)

23. Shen, J., Xu, J., Yang, J.: A new class of efficient and robust energy stable schemes for gradient flows. SIAM Rev. **61**(3), 474–506 (2019). https://doi.org/10.1137/17M1150153

24. Yang, Z., Dong, S.: An unconditionally energy-stable scheme based on an implicit auxiliary energy variable for incompressible two-phase flows with different densities involving only precomputable coefficient matrices. J. Comput. Phys. **393**, 229–257 (2019). https://doi.org/10.1016/j.jcp.2019.05.018

25. Yang, Z., Dong, S.: A roadmap for discretely energy-stable schemes for dissipative systems based on a generalized auxiliary variable with guaranteed positivity. J. Comput. Phys. **404**, 109121–46 (2020). https://doi.org/10.1016/j.jcp.2019.109121

26. Yang, X.: A novel fully-decoupled, second-order and energy stable numerical scheme of the conserved Allen–Cahn type flow-coupled binary surfactant model. Comput. Methods Appl. Mech. Eng. **373**, 113502 (2021). https://doi.org/10.1016/j.cma.2020.113502

27. Li, S.J. Xiaoli, Liu, Z.: New sav-pressure correction methods for the Navier–Stokes equations: stability and error analysis. Math. Comput. https://doi.org/10.1090/mcom/3651 (2021)

28. Jiang, N., Yang, H.: SAV decoupled ensemble algorithms for fast computation of Stokes–Darcy flow ensembles. Comput. Methods Appl. Mech. Eng. **387**, 34–114150 (2021). https://doi.org/10.1016/j.cma.2021.114150

29. Labovsky, A., Layton, W.J., Manica, C.C., Neda, M., Rebholz, L.G.: The stabilized extrapolated trapezoidal finite-element method for the Navier–Stokes equations. Comput. Methods Appl. Mech. Engrg. **198**(9–12), 958–974 (2009). https://doi.org/10.1016/j.cma.2008.11.004

30. Li, X., Wang, W., Shen, J.: Stability and error analysis of IMEX SAV schemes for the magneto-hydrodynamic equations. SIAM J. Numer. Anal. **60**(3), 1026–1054 (2022). https://doi.org/10.1137/21M1430376

31. Zhang, C., Ouyang, J., Wang, C., Wise, S.M.: Numerical comparison of modified-energy stable SAV-type schemes and classical BDF methods on benchmark problems for the functionalized Cahn–Hilliard equation. J. Comput. Phys. **423**, 35–109772 (2020). https://doi.org/10.1016/j.jcp.2020.109772

32. Jiang, M., Zhang, Z., Zhao, J.: Improving the accuracy and consistency of the scalar auxiliary variable (SAV) method with relaxation. J. Comput. Phys. **456**, 110954 (2022). https://doi.org/10.1016/j.jcp.2022.110954

33. Foias, C., Holm, D.D., Titi, E.S.: The Navier–Stokes-alpha model of fluid turbulence. vol. 152/153, pp. 505–519 (2001). https://doi.org/10.1016/S0167-2789(01)00191-9. Advances in nonlinear mathematics and science. https://doi-org.libproxy.mst.edu/10.1016/S0167-2789(01)00191-9

34. Chen, S., Holm, D.D., Margolin, L.G., Zhang, R.: Direct numerical simulations of the Navier-Stokes alpha model. **133**, 66–83 (1999) Predictability: quantifying uncertainty in models of complex phenomena (Los Alamos, NM, 1998). https://doi.org/10.1016/S0167-2789(99)00099-8

35. Wang, C., Wang, J., Xia, Z., Xu, L.: Optimal error estimates of a Crank–Nicolson finite element projection method for magnetohydrodynamic equations. ESAIM Math. Model. Numer. Anal. **56**(3), 767–789 (2022). https://doi.org/10.1051/m2an/2022020

36. Li, B., Wang, J., Xu, L.: A convergent linearized Lagrange finite element method for the magneto-hydrodynamic equations in two-dimensional nonsmooth and nonconvex domains. SIAM J. Numer. Anal. **58**(1), 430–459 (2020). https://doi.org/10.1137/18M1205649

37. Li, B., Ma, S., Ueda, Y.: Analysis of fully discrete finite element methods for 2D Navier–Stokes equations with critical initial data. ESAIM Math. Model. Numer. Anal. **56**(6), 2105–2139 (2022). https://doi.org/10.1051/m2an/2022073

38. Li, B., Ma, S., Wang, N.: Second-order convergence of the linearly extrapolated Crank–Nicolson method for the Navier–Stokes equations with H^1 initial data. J. Sci. Comput. **88**(3), 20–70 (2021). https://doi.org/10.1007/s10915-021-01588-8

39. Gunzburger, M.D.: Finite element methods for viscous incompressible flows. Computer Science and Scientific Computing. Academic Press, San Diego (1989). https://doi.org/10.1016/B978-0-12-307350-1.50002-8. https://www.sciencedirect.com/science/article/pii/B9780123073501500028

40. Brenner, S., Scott, R.: The Mathematical Theory of Finite Element Methods. Texts in Applied Mathematics. Springer (2007). https://books.google.com/books?id=ci4c_R0WKYYC

41. Kraichnan, R.H.: Inertial ranges in two-dimensional turbulence. Phys. Fluids **10**(7), 1417–1423 (1967). https://doi.org/10.1063/1.1762301

42. Alnæs, M., Blechta, J., Hake, J., Johansson, A., Kehlet, B., Logg, A., Richardson, C., Ring, J., Rognes, M., Wells, G.: The fenics project version 1.5 **3** (2015). https://doi.org/10.11588/ans.2015.100.20553

43. Zhang, G., He, X., Yang, X.: Fully decoupled, linear and unconditionally energy stable time discretization scheme for solving the magneto-hydrodynamic equations. J. Comput. Appl. Math. **369**, 112636 (2019). https://doi.org/10.1016/j.cam.2019.112636